DYNAMICS OF VORTICES IN TWO-DIMENSIONAL BOSE-EINSTEIN CONDENSATES

Shu-Ming Chang*, Tai-Chia Lin†, and Wen-Wei Lin‡
† *Department of Mathematics, Chung Cheng U., Chiayi 621, Taiwan*
‡ *Department of Mathematics, Tsing Hua U., Hsingchu 300, Taiwan*

Abstract

We derive the asymptotic motion equations of vortices for the time-dependent Gross-Pitaevskii equation with a harmonic trap potential. The asymptotic motion equations form a system of ordinary differential equations which can be regarded as a perturbation of the standard Kirchhoff problem. From the numerical simulation on the asymptotic motion equations, we observe that the bounded and collisionless trajectories of three vortices form chaotic, quasi 2- or quasi 3-periodic orbits. Furthermore, a new phenomenon of 1 : 1-topological synchronization is observed in the chaotic trajectories of two vortices.

1 Introduction

In this paper, we study the time-dependent Gross-Pitaevskii equation given by

$$-i\,u_t = \Delta u - V_\epsilon(x,y)\,u + \frac{1}{\epsilon^2}(1-|u|^2)\,u \quad \text{for } (x,y)\in\mathbb{R}^2, t>0, \tag{1.1}$$

with the initial data

$$u|_{t=0} = u_0(x,y) \quad \text{for } (x,y)\in\mathbb{R}^2, \tag{1.2}$$

where u is a complex-valued order parameter and ϵ is a positive small parameter. Hereafter, $V_\epsilon(x,y) = \alpha_\epsilon\,x^2 + \beta_\epsilon\,y^2$ is a harmonic trap potential in a two-dimensional Bose-Einstein condensate, where α_ϵ and β_ϵ are positive constants depending on ϵ. The time-dependent Gross-Pitaevskii equation was introduced as a phenomenological equation for the order parameter in superfluids. Due to recent experiments on Bose-Einstein condensation of dilute

*m863254@am.nthu.edu.tw
†tclin@math.ccu.edu.tw
‡wwlin@am.nthu.edu.tw

gases in magnetic traps, the time-dependent Gross-Pitaevskii equation has become a well-known model to describe a trapped Bose-Einstein condensate (see Dalfovo *et al.* [1999]).

Vortices and their motions have long been an important phenomenon in superfluids and Bose-Einstein condensates. In superfluids, the circulation in a vortex must be quantized, i.e., in a closed path around the vortex, the phase undergoes a $\pm 2\pi$ winding. Mean-field theories, which are based on the Bogoliubov approximation [Bogoliubov, 1947], predict that a continuum Bose-Einstein condensate with repulsive interactions should be a superfluid and it can exhibit quantized vortices [Feder *et al.*, 1999]. Recently, quantized vortices in a Bose-Einstein condensate have been observed in experiments (cf. [Matthews *et al.*, 1999; Madison *et al.*, 2000]). For the dynamics of a vortex in a Bose-Einstein condensate, Lundh and Ao [2000] used the hydrodynamic approach and found that an off-center vortex will move in a circular trajectory around the trap center. Svidzinsky and Fetter [preprint] investigated the dynamic law of a vortex by the formal asymptotic analysis. However, the communication of multiple vortices is still unknown. In this paper, we will study a general result on the dynamics of vortices in trapped Bose-Einstein condensates.

One of our main results is to derive the dynamics of vortices in trapped Bose-Einstein condensates. Suppose the initial data u_0 in (1.2) has $d \in \mathbb{N}$ vortex centers at $q_j(0), j = 1, \cdots, d$ with winding numbers $n_j \in \{\pm 1\}, j = 1, \cdots, d$. For the stability of the vortex structure in u, we require $n_j \in \{\pm 1\}, j = 1, \cdots, d$. Under some specific assumptions on u_0, we may derive the asymptotic motion equations of d vortices q_j's in the following:

Case 1. Assume that $\alpha_\epsilon, \beta_\epsilon \sim \epsilon^{-2} (\log \frac{1}{\epsilon})^{-1}$, i.e., $\alpha_\epsilon = \epsilon^{-2} (\log \frac{1}{\epsilon})^{-1} (\alpha_0 + o_\epsilon(1)), \beta_\epsilon = \epsilon^{-2} (\log \frac{1}{\epsilon})^{-1} (\beta_0 + o_\epsilon(1))$, where α_0 and β_0 are positive constants independent of ϵ, and $o_\epsilon(1)$ is a small quantity which tends to zero as ϵ goes to zero. Then the asymptotic motion equations of d vortices q_j's are

$$\begin{aligned} n_j \, \dot{q}_{jx} &= -\partial_{q_{jy}} W(q_1, \cdots, q_d) - 2\, n_j \, \beta_0 \, q_{jy} \,, \\ n_j \, \dot{q}_{jy} &= \quad \partial_{q_{jx}} W(q_1, \cdots, q_d) + 2\, n_j \, \alpha_0 \, q_{jx} \,, \end{aligned} \tag{1.3}$$

for $j = 1, \cdots, d$.

Case 2. Assume that $\alpha_\epsilon, \beta_\epsilon \ll \epsilon^{-2} (\log \frac{1}{\epsilon})^{-1}$, i.e., $\alpha_\epsilon, \beta_\epsilon = o_\epsilon(1)\, \epsilon^{-2} (\log \frac{1}{\epsilon})^{-1}$, where $o_\epsilon(1)$ is a small quantity which tends to zero as ϵ goes to zero. Then the asymptotic motion equations of d vortices q_j's are

$$\begin{aligned} n_j \, \dot{q}_{jx} &= -\partial_{q_{jy}} W(q_1, \cdots, q_d) \,, \\ n_j \, \dot{q}_{jy} &= \quad \partial_{q_{jx}} W(q_1, \cdots, q_d) \,, \end{aligned} \tag{1.4}$$

for $j = 1, \cdots, d$.

Case 3. Assume that $\alpha_\epsilon, \beta_\epsilon \gg \epsilon^{-2} (\log \frac{1}{\epsilon})^{-1}$, i.e., $\alpha_\epsilon = \lambda_\epsilon \, \alpha_0 \,, \beta_\epsilon = \lambda_\epsilon \, \beta_0$ and $\lambda_\epsilon \, \epsilon^2 \, \log \frac{1}{\epsilon} \to \infty$ as $\epsilon \to 0+$. Then under a suitable time scale $O(\lambda_\epsilon \, \epsilon^2 \, \log \frac{1}{\epsilon})$, the asymptotic motion

equations of d vortices q_j's are

$$\dot{q}_{jx} = -2\,\beta_0\,q_{jy}\,, \quad \dot{q}_{jy} = 2\,\alpha_0\,q_{jx}\,, \quad j = 1, \cdots, d\,, \tag{1.5}$$

where $q_j = q_j(t) = (q_{jx}(t), q_{jy}(t))$, and

$$W = \sum_{\substack{j,\,k\,=\,1\\ j\,\neq\,k}}^{d} n_j\,n_k\,\log|q_j - q_k|\,. \tag{1.6}$$

For the vortex dynamics in superfluids, the governing equation is given by

$$\begin{cases} -i\,u_t = \Delta u + \frac{1}{\epsilon^2}(1 - |u|^2)u & \text{for } (x,y) \in \mathbb{R}^2\,, t > 0\,, \\ u|_{t=0} = u_0(x,y) & \text{for } (x,y) \in \mathbb{R}^2\,, \end{cases} \tag{1.7}$$

where ϵ is a positive small parameter, u is a complex-valued order parameter and the initial data u_0 has $d \in \mathbb{N}$ vortex centers at $q_j(0), j = 1, \cdots, d$ with winding numbers $n_j \in \{\pm 1\}, j = 1, \cdots, d$. For the stability of the vortex structure in u, we require $n_j \in \{\pm 1\}, j = 1, \cdots, d$. The equation (1.7) is the Gross-Pitaevskii equation for superfluids (cf. [Donnelly, 1991; Frisch *et al.*, 1992; Ginzburg & Pitaevskii, 1958; Josserand & Pomeau, 1995; Landau & Lifschitz, 1989; Nozieres & Pines, 1990]). From [E, 1994], [Lin & Xin, 1999] and [Neu, 1990], the asymptotic motion equations of d vortices q_j's form the system (1.4).

To distinguish the dynamics of (1.3) and (1.4), we study the long-time dynamics of (1.3) and (1.4) with $d = 3$ by numerical simulations. The system (1.4) is the Kirchhoff problem which is a standard problem for the motion of vortices in fluid mechanics (cf. Kirchhoff [1883]). From Aref [1979, 1983], the Kirchhoff problem (1.4) is an integrable system if $d \leq 3$, and it may have chaotic motions in a bounded region if $d \geq 4$. Hence the bounded and collisionless trajectories of the system (1.4) with $d = 3$ are either periodic or quasiperiodic. The system (1.3) can be regarded as a perturbation of the system (1.4). Moreover, the system (1.3) has the same nonlinear terms as the system (1.4). However, by the numerical simulation on the system (1.3) with $d = 3$, we may observe chaotic motions of q_j's in a bounded region for some α_0 and β_0. Hence it is possible that the dynamics of three vortices in two-dimensional Bose-Einstein condensates may have chaotic motions in a bounded region. This may provide a difference between Bose-Einstein condensates and superfluids.

We may rewrite the system (1.3) with $d = 3$ as follows:

$$\begin{aligned} \dot{q}_{jx} &= -\sum_{\substack{k\,=\,1\\ k\,\neq\,j}}^{d} n_k\,\frac{q_{jy} - q_{ky}}{|q_j - q_k|^2} - \omega_1\,q_{jy}\,, \\ \dot{q}_{jy} &= \sum_{\substack{k\,=\,1\\ k\,\neq\,j}}^{d} n_k\,\frac{q_{jx} - q_{kx}}{|q_j - q_k|^2} + \omega_2\,q_{jx}\,, \end{aligned} \tag{1.8}$$

for $j = 1, \cdots, d$, where $\omega_1 = 2\beta_0$ and $\omega_2 = 2\alpha_0$. Generically, we may set ω_1, ω_2 to be any real numbers (see Remark 3 in Section 2). From numerical experiments, we observe that

the bounded and collisionless trajectories of three vortices form chaotic orbits, quasi 2- or 3-periodic solutions. Furthermore, we obtain a new phenomenon of 1 : 1-topological synchronization on two chaotic trajectories of vortices. Actually, this topological synchronization is of frequency synchronization but not of identical synchronization, phase synchronization and lag synchronization.

The rest of this paper is organized as follows. In Section 2, we derive the system (1.3) for the asymptotic motion equations of vortices. The main tool of our argument is the spectrum of the linearized operator for the steady state equation of (1.7) with respect to the symmetric vortex solution of the steady state equation of (1.7). In Section 3, we state the numerical results on the system (1.8).

2 Vortex Dynamics in Bose-Einstein Condensates

For the dynamics of a single vortex, we assume that the solution u of (1.1) has only one vortex center at $\mathrm{q(t)}$, where $\mathrm{q(t)} = (\mathrm{q_x(t)}, \mathrm{q_y(t)})$ is smooth in t, and $B_{r_0}(\mathrm{q(t)})$ is the vortex core which moves along with the vortex trajectory $(x, y) = \mathrm{q(t)}$. Here $B_{r_0}(\mathrm{q(t)})$ is a disk on $\mathbb{R}^2$ with radius r_0 and center at $\mathrm{q(t)}$, where r_0 is a positive constant independent of ϵ. Moreover, there is an essential hypothesis given by

Main Hypothesis. When a vortex begins to move at the time $t = 0$, the vortex structure on the vortex core $B_{r_0}(\mathrm{q})$ does not change much at the time $t = 0$.
Main Hypothesis is to preserve the vortex structure on the vortex core when the vortex moves. We will use Assumption 2.1 in the middle part of this section to fulfill Main Hypothesis and derive the vortex dynamics.

Now we focus on the vortex core $B_{r_0}(\mathrm{q})$ and consider the following system of equations:

$$\begin{cases} -i\,u_t = \Delta u - V_\epsilon(x,y)\,u + \frac{1}{\epsilon^2}\,(1-|u|^2)\,u & \text{for } (x,y) \in B_{r_0}(\mathrm{q(t)}),\ \mathrm{t} > 0, \\ u|_{t=0} = u_0(x,y) & \text{for } (x,y) \in B_{r_0}(\mathrm{q(0)})\,. \end{cases} \tag{2.1}$$

We introduce the stretched variables

$$\mathbb{X} = \frac{x - \mathrm{q_x(t)}}{\epsilon}, \quad \mathbb{Y} = \frac{y - \mathrm{q_y(t)}}{\epsilon}, \tag{2.2}$$

and we set

$$\Psi(\mathbb{X}, \mathbb{Y}, t, \epsilon) = u(x, y, t, \epsilon)$$

for $(x, y) \in B_{r_0}(\mathrm{q})$, i.e., $(\mathbb{X}, \mathbb{Y}) \in B_{r_0/\epsilon}(0)$. From (2.2), the trap potential $V_\epsilon(x, y) = \alpha_\epsilon\, x^2 + \beta_\epsilon\, y^2$ can be written by

$$V_\epsilon(x,y) = 2\epsilon(\alpha_\epsilon\,\mathrm{q_x}\,\mathbb{X} + \beta_\epsilon\,\mathrm{q_y}\,\mathbb{Y}) + [\alpha_\epsilon(\mathrm{q_x^2} + \epsilon^2\mathbb{X}^2) + \beta_\epsilon(\mathrm{q_y^2} + \epsilon^2\mathbb{Y}^2)]\,. \tag{2.3}$$

Then by (2.1) and (2.3), we have

$$\begin{cases} -i\,\epsilon^2\,\Psi_t = -i\,\epsilon\,\dot{\mathrm{q}}\cdot\tilde{\nabla}\,\Psi + \tilde{\Delta}\,\Psi + (1-|\Psi|^2)\,\Psi \\ \qquad\qquad - \epsilon^2\,\{2\epsilon(\alpha_\epsilon\,\mathrm{q_x}\,\mathbb{X} + \beta_\epsilon\,\mathrm{q_y}\,\mathbb{Y}) + [\alpha_\epsilon(\mathrm{q_x^2} + \epsilon^2\mathbb{X}^2) + \beta_\epsilon(\mathrm{q_y^2} + \epsilon^2\mathbb{Y}^2)]\}\,\Psi \\ \qquad\qquad\quad \text{for } (\mathbb{X},\mathbb{Y}) \in B_{r_0/\epsilon}(0),\ t > 0, \\ \Psi|_{t=0} \quad = u_0 \quad \text{for } (\mathbb{X},\mathbb{Y}) \in B_{r_0/\epsilon}(0)\,, \end{cases} \tag{2.4}$$

where

$$\tilde{\nabla} = (\partial_{\mathbb{X}}, \partial_{\mathbb{Y}}), \quad \tilde{\Delta} = \partial_{\mathbb{X}}^2 + \partial_{\mathbb{Y}}^2, \tag{2.5}$$

and $\Psi_t = \frac{\partial}{\partial t}\Psi(\cdot,\cdot,t,\epsilon)$. We take an expansion form of Ψ as follows.

$$\Psi(\mathbb{X},\, \mathbb{Y},\, t,\, \epsilon) = \Psi_0(\mathbb{X},\mathbb{Y})\, e^{i\,H} + \epsilon\, \Psi_1(\mathbb{X},\, \mathbb{Y},\, t,\, \epsilon)\, e^{i\,H}, \tag{2.6}$$

where $\Psi_0 = \Psi_0(\mathbb{X},\mathbb{Y})$ satisfies that

$$\Psi_0(\mathbb{X},\mathbb{Y}) = f_0(R)\, e^{i\,\theta}, \quad R = |(\mathbb{X},\mathbb{Y})|, \quad \theta = \arg(\mathbb{X},\mathbb{Y}), \tag{2.7}$$

and $f_0(R)$ is the solution of

$$\begin{cases} -f'' - \dfrac{1}{R}\, f' + \dfrac{1}{R^2}\, f = (1-f^2)\, f \quad \text{for } R>0, \\ \\ \quad f(+\infty) = 1, \quad f(0) = 0, \quad f \geq 0. \end{cases} \tag{2.8}$$

From [Chen *et al.*, 1994], [Hagan, 1982] and [Hervé & Hervé, 1994], we learned that (2.8) has a unique solution and Ψ_0 is called the symmetric vortex solution of the steady state equation of (1.7) in $\mathbb{R}^2$. In addition, we assume that $H = H(x,y,t,\epsilon)$ is a smooth real-valued function and satisfies

$$\Delta H = 0, \quad |\nabla H|, |H_t|, |\nabla H_t| \leq K \quad \text{for } (x,y) \in B_{r_0}(\mathrm{q(t)}),\ \mathrm{t} > 0, \tag{2.9}$$

where $H_t = \frac{\partial}{\partial t} H$ and K is a positive constant independent of ϵ.

By (2.6)–(2.9), (2.4) becomes

$$\begin{aligned} &-i\,\dot{\mathrm{q}}\cdot(\tilde{\nabla}\Psi_0 + \epsilon\tilde{\nabla}\Psi_1) - \epsilon\Psi_0\, H_t - \epsilon^2\Psi_1\, H_t + i\,\epsilon^2\,\Psi_{1,\,t} \\ &= \epsilon\Psi_0\,|\nabla H|^2 - 2i(\tilde{\nabla}\Psi_0\,\cdot\,\nabla H) + \tilde{L}_\epsilon(\Psi_1) + \hat{N}_\epsilon(\Psi_1) \\ &\quad + \epsilon\left\{2\epsilon(\alpha_\epsilon\,\mathrm{q_x}\,\mathbb{X} + \beta_\epsilon\,\mathrm{q_y}\,\mathbb{Y}) + [\alpha_\epsilon(\mathrm{q_x^2} + \epsilon^2\mathbb{X}^2) + \beta_\epsilon(\mathrm{q_y^2} + \epsilon^2\mathbb{Y}^2)]\right\}(\Psi_0 + \epsilon\Psi_1) \\ &\quad \text{for } (\mathbb{X},\mathbb{Y}) \in B_{r_0/\epsilon}(0),\ t > 0, \end{aligned} \tag{2.10}$$

where

$$\begin{cases} -\tilde{L}_\epsilon(\Psi_1) = \tilde{\Delta}\,\Psi_1 + (1 - |\Psi_0|^2)\Psi_1 - 2(\Psi_0\,\cdot\,\Psi_1)\Psi_0, \\ \hat{N}_\epsilon(\Psi_1) = \epsilon^2\Psi_1|\nabla H|^2 - 2i\epsilon(\tilde{\nabla}\Psi_1\,\cdot\,\nabla H) + \epsilon^2\,|\Psi_1|^2\,\Psi_1 \\ \qquad\qquad + \epsilon[\,2(\Psi_0\cdot\Psi_1)\Psi_1 + |\Psi_1|^2\Psi_0\,], \end{cases} \tag{2.11}$$

and $\Psi_{1,\,t} = \frac{\partial}{\partial t}\Psi_1(\cdot\,,t\,,\epsilon)$. Note that in the first term of (2.11), $(\Psi_0\cdot\Psi_1) = \frac{1}{2}(\bar{\Psi}_0\Psi_1 + \bar{\Psi}_1\Psi_0)$ and $\bar{(\cdot)}$ denotes as the complex conjugate.

The spectrum information of the linear operator $\tilde{L}_\epsilon$ is essential for our argument. From Lin [1997, 2000], we have estimates on the eigenvalues of $\tilde{L}_\epsilon$ as follows.

Theorem 2.1 *Let λ_1 and λ_2 be the first and the second eigenvalue of $\tilde{L}_\epsilon$. Then*

(i) *the eigenvalue λ_1 has only two associated eigenfunctions $\tilde{e}_1 = a_\epsilon(R) + b_\epsilon(R)\, e^{2i\,\theta}$ and $\tilde{e}_2 = ia_\epsilon(R) - ib_\epsilon(R)\, e^{2i\,\theta}$, where a_ϵ and b_ϵ are real-valued.*

(ii) $0 < \lambda_1 = O(\epsilon^2(\log \frac{r_0}{\epsilon})^{-1})$ *as* $\epsilon \to 0+$.

(iii) there exist $\epsilon_1 > 0$ *and* $c_1 > 0$ *independent of* ϵ *such that* $\lambda_2 \geq \epsilon^2\, c_1$ *for* $0 < \epsilon \leq \epsilon_1$.

Let

$$\tilde{w}_1 = \frac{\partial_{\mathbb{X}} \Psi_0}{\|\partial_{\mathbb{X}} \Psi_0\|_{L^2}}\,, \quad \tilde{w}_2 = \frac{\partial_{\mathbb{Y}} \Psi_0}{\|\partial_{\mathbb{Y}} \Psi_0\|_{L^2}}\,, \tag{2.12}$$

where $\|\cdot\|_{L^2}$ is the L^2 norm on the disk $B_{\frac{r_0}{\epsilon}}(0)$. We observe that $\tilde{w}_j$'s are from the translation invariance. In Lin [2000], we used Theorem 2.1 to derive a useful estimate of eigenfunctions $\tilde{e}_j$'s as follows.

Proposition 2.1 *Assume that*

$$\langle \tilde{w}_j, \tilde{e}_j \rangle > 0, \quad \|\tilde{e}_j\|_{L^2} = 1\,, \quad j = 1, 2\,.$$

Then the eigenfunctions $\tilde{e}_j$*'s satisfy*

$$\tilde{e}_j = \tilde{w}_j + \nu_{j,\epsilon}\,, \quad \|\nu_{j,\epsilon}\|_{L^2} = O((\log \frac{1}{\epsilon})^{-\frac{1}{2}}) \quad \text{as } \epsilon \to 0+\,, \ \text{for } j = 1, 2.$$

Hereafter, we use $\|\cdot\|_{L^2}$ and $\langle \cdot, \cdot \rangle$ to denote the L^2 norm and the L^2 inner product respectively on the disk $B_{\frac{r_0}{\epsilon}}(0)$. Let $\tilde{V}_1 = \{a(R) + b(R)\, e^{2i\theta} \in H_0^1(B_{\frac{r_0}{\epsilon}}(0)\,; \mathbb{C})\}$. Then it is easy to check that $\tilde{V}_1$ is invariant under $\tilde{L}_\epsilon^{-1}$. Hence we set $\tilde{e}_{j,k} \in \tilde{V}_1$'s the unit L^2 norm eigenfunctions of $\tilde{L}_\epsilon$ corresponding to the eigenvalue $\tilde{\lambda}_k$ respectively for $k \geq 2$. Then $\tilde{e}_j$'s and $\tilde{e}_{j,k}$'s are dense in $V_1 = \{a(R) + b(R)\, e^{2i\theta} \in L^2(B_{\frac{r_0}{\epsilon}}(0)\,; \mathbb{C})\}$. Since $\tilde{w}_l \in V_1, l = 1, 2$, then $\tilde{w}_l$'s can be represented by $\tilde{e}_j$'s and $\tilde{e}_{j,k}$'s as follows.

$$\tilde{w}_l = \sum_{j=1}^{2} \langle \tilde{w}_l, \tilde{e}_j \rangle \tilde{e}_j \ + \sum_{k=2}^{\infty} \sum_{j=1}^{J(k)} \langle \tilde{w}_l, \tilde{e}_{j,k} \rangle \tilde{e}_{j,k}\,, \tag{2.13}$$

where $J(k)$ is the multiplicity of the eigenvalue $\tilde{\lambda}_k, k \geq 2$. Using integration by parts, we have

$$\begin{cases} \langle \tilde{L}_\epsilon(\Psi_1)\,, \tilde{e}_j \rangle &= \displaystyle\int_{\partial B_{r_0/\epsilon}(0)} \Psi_1 \cdot \partial_{\hat{n}} \tilde{e}_j + \lambda_1 \langle \Psi_1\,, \tilde{e}_j \rangle\,, \\ \langle \tilde{L}_\epsilon(\Psi_1)\,, \tilde{e}_{j,k} \rangle &= \displaystyle\int_{\partial B_{r_0/\epsilon}(0)} \Psi_1 \cdot \partial_{\hat{n}} \tilde{e}_{j,k} + \tilde{\lambda}_k \langle \Psi_1\,, \tilde{e}_{j,k} \rangle\,, \end{cases} \tag{2.14}$$

where $\partial_{\hat{n}}$ is the normal derivative. Hereafter, $(\alpha \cdot \beta) \equiv \frac{1}{2}(\bar{\alpha}\beta + \bar{\beta}\alpha)$ for $\alpha, \beta \in \mathbb{C}$. Here we have used the fact that the eigenfunctions $\tilde{e}_j, \tilde{e}_{j,k} \in H_0^1(B_{\frac{r_0}{\epsilon}}(0)\,; \mathbb{C})$. Then all the terms $\int_{\partial B_{\frac{r_0}{\epsilon}}(0)} \tilde{e}_j \cdot \partial_{\hat{n}} \Psi_1$ and $\int_{\partial B_{\frac{r_0}{\epsilon}}(0)} \tilde{e}_{j,k} \cdot \partial_{\hat{n}} \Psi_1$ in (2.14) become zero. Hence by (2.13), (2.14) and Proposition 2.1, we obtain

$$\begin{aligned} \langle \tilde{L}_\epsilon(\Psi_1)\,, \tilde{w}_l \rangle &= \sum_{j=1}^{2} \left[\lambda_1 \langle \Psi_1\,, \tilde{e}_j \rangle + \int_{\partial B_{r_0/\epsilon}(0)} \Psi_1 \cdot \partial_{\hat{n}} \tilde{e}_j \right] \langle \tilde{w}_l\,, \tilde{e}_j \rangle \\ &\quad + \sum_{k=2}^{\infty} \sum_{j=1}^{J(k)} \left[\tilde{\lambda}_k \langle \Psi_1\,, \tilde{e}_{j,k} \rangle + \int_{\partial B_{r_0/\epsilon}(0)} \Psi_1 \cdot \partial_{\hat{n}} \tilde{e}_{j,k} \right] \langle \tilde{w}_l\,, \tilde{e}_{j,k} \rangle \\ &= o_\epsilon((\log \tfrac{1}{\epsilon})^{-\frac{1}{2}})\,, \quad l = 1, 2\,, \end{aligned} \tag{2.15}$$

provided that Ψ_1 satisfies

$$\begin{aligned} &|\langle \Psi_1 \, , \tilde{e}_j \rangle| && = o_\epsilon(\epsilon^{-2}(\log \tfrac{1}{\epsilon})^{1/2}) \, , j = 1, 2 \, , \\ &\sum_{k=2}^{\infty} \sum_{j=1}^{J(k)} \epsilon^2 \lambda_k \, |\langle \Psi_1 \, , \tilde{e}_{j \, , k} \rangle| && = o_\epsilon(1) \, , \end{aligned} \tag{2.16}$$

$$\begin{aligned} &\left| \int_{\partial B_{\frac{r_0}{\epsilon}}(0)} \Psi_1 \cdot \partial_{\vec{n}} \, \tilde{e}_j \right| && = o_\epsilon((\log \tfrac{1}{\epsilon})^{-1/2}) \, , j = 1, 2 \, , \\ &\sum_{k=2}^{\infty} \sum_{j=1}^{J(k)} \left| \int_{\partial B_{\frac{r_0}{\epsilon}}(0)} \Psi_1 \cdot \partial_{\vec{n}} \, \tilde{e}_{j \, , k} \right| && = o_\epsilon(1) \, , \end{aligned} \tag{2.17}$$

where $K > 0$ is a constant and $\partial_{\vec{n}}$ is the normal derivative. Hereafter, we denote $o_\epsilon(1)$ as a small quantity, independent of time t, and tending to zero as $\epsilon \to 0+$.

The main idea of the proof of vortex dynamics is to make the L^2 inner product with (2.10) and $\tilde{w}_j, j = 1, 2$. We require that Ψ_1 satisfies the "small" perturbation condition (2.16), (2.17) and

$$\begin{aligned} &\|\tilde{\nabla} \Psi_1\|_{L^2(B_{r_0/\epsilon}(0))} && \leq K \epsilon^{-\beta} \, , && 0 < \beta < 1 \, , \\ &\|\Psi_1\|_{L^6(B_{r_0/\epsilon}(0))} && \leq K \epsilon^{-\gamma} \, , && 0 < \gamma < \tfrac{1}{3} \, , \\ &\|\Psi_1\|_{L^2(B_{r_0/\epsilon}(0))} && = o_\epsilon((\log \tfrac{1}{\epsilon})^{\frac{1}{2}}) \, , \\ &\|\Psi_{1 \, , t}\|_{L^2(B_{r_0/\epsilon}(0))} && \leq K \epsilon^{-\delta} \, , && 0 < \delta < 2 \, , \end{aligned} \tag{2.18}$$

Note that the upper bound of (2.18) and the first term of (2.16) tend to infinity as ϵ goes to zero. From Haraux [1981], the equation (1.1) is well posed. Then Ψ_1 is smooth in both space and time variables. Hence (2.16), (2.17) and (2.18) can be fulfilled at least in a short time when $\Psi_1|_{t=0}$ satisfies

Assumption 2.1 $\Psi_1 = \Psi_1(\mathbb{X}, \mathbb{Y}, t, \epsilon)$ *satisfies*

(a) $\Psi_1(\cdot, \cdot, 0, \epsilon)$ *has sufficiently small* C^1 *norm on the vortex core* $(\mathbb{X}, \mathbb{Y}) \in B_{r_0/\epsilon}(0)$ *at* $t = 0$,

(b) $\|\partial_t \Psi_1(\cdot, \cdot, 0, \epsilon)\|_{L^2(B_{r_0/\epsilon}(0))} = O(\epsilon^{-\delta}), 0 < \delta < 2$.

By the suitable choice of initial data u_0, we obtain Assumption 2.1(a). Assumption 2.1(b) preserves the vortex structure on the vortex core when the associated vortex point begins to move at the time $t = 0$. Note that the upper bound of Assumption 2.1(b) is $\sim \epsilon^{-\delta}, 0 < \delta < 2$ which tends to infinity as ϵ goes to zero. Actually, Assumption 2.1 which may assure (2.16), (2.17) and (2.18) is more generalized than the assumptions of the standard asymptotic analysis. To derive the dynamics of vortices, the standard asymptotic analysis is well-accepted (cf. [E, 1994; Neu, 1990; Ting & Klein, 1991]). In E [1994] and Neu [1990], E and Neu used a specific asymptotic expansion formula and some pointwise conditions for the solution on vortex cores to derive the dynamics of vortices. However, (2.16), (2.17) and (2.18) are not pointwise. This is a kind of generalization for the assumptions of the standard asymptotic analysis.

Now we derive the vortex dynamics as follows. Making the inner product with (2.10) and $\tilde{w}_j, j = 1, 2$ and using (2.15), we have

$$\begin{aligned} &-\dot{q}_x \left[\langle i\partial_{\mathbb{X}}\Psi_0\,,\tilde{w}_j\rangle + \epsilon\langle i\partial_{\mathbb{X}}\Psi_1\,,\tilde{w}_j\rangle\right] - \dot{q}_y\left[\langle i\partial_{\mathbb{Y}}\Psi_0\,,\tilde{w}_j\rangle + \epsilon\langle i\partial_{\mathbb{Y}}\Psi_1\,,\tilde{w}_j\rangle\right] \\ &= \hat{\Gamma}_j \,+\, \epsilon^2\left(\langle i\Psi_{1,t}\,,\tilde{w}_j\rangle \,+\, \langle\Psi_1 H_t\,,\tilde{w}_j\rangle\right) \,+\, \langle\hat{N}_\epsilon(\Psi_1)\,,\tilde{w}_j\rangle + o_\epsilon\left((\log\tfrac{1}{\epsilon})^{-1/2}\right) \end{aligned} \tag{2.19}$$

where

$$\begin{aligned} \hat{\Gamma}_j \;=\; &-2\langle i\partial_{\mathbb{X}}\,\Psi_0\,\partial_x H\,,\tilde{w}_j\rangle \,-\, 2\langle i\partial_{\mathbb{Y}}\,\Psi_0\,\partial_y H\,,\tilde{w}_j\rangle \\ &+\, \epsilon\langle\Psi_0|\nabla H|^2\,,\tilde{w}_j\rangle \,+\, \epsilon\langle\Psi_0 H_t\,,\tilde{w}_j\rangle \\ &+\, 2\epsilon^2[\alpha_\epsilon\,\mathrm{q_x}\,\langle\mathbb{X}(\Psi_0+\epsilon\Psi_1)\,,\tilde{\mathrm{w}}_\mathrm{j}\rangle + \beta_\epsilon\,\mathrm{q_y}\,\langle\mathbb{Y}(\Psi_0+\epsilon\Psi_1)\,,\tilde{\mathrm{w}}_\mathrm{j}\rangle] \\ &+\, \epsilon\,(\alpha_\epsilon\mathrm{q_x}^2+\beta_\epsilon\mathrm{q_y}^2)\langle(\Psi_0+\epsilon\Psi_1)\,,\tilde{\mathrm{w}}_\mathrm{j}\rangle + \epsilon^3\,\langle(\alpha_\epsilon\mathbb{X}^2+\beta_\epsilon\mathbb{Y}^2)\,(\Psi_0+\epsilon\Psi_1)\,,\tilde{\mathrm{w}}_\mathrm{j}\rangle\,. \end{aligned} \tag{2.20}$$

It is easy to check that

$$\begin{aligned} \partial_{\mathbb{X}}\,\Psi_0 &= \tfrac{1}{2}(\tfrac{1}{s}f_0 \,+\, f_0') \,+\, \tfrac{1}{2}(f_0' \,-\, \tfrac{1}{s}f_0)\,e^{2i\,\phi}\,, \\ \partial_{\mathbb{Y}}\,\Psi_0 &= \tfrac{i}{2}(\tfrac{1}{s}f_0 \,+\, f_0') \,+\, \tfrac{i}{2}(\tfrac{1}{s}f_0 \,-\, f_0')\,e^{2i\,\phi}\,. \end{aligned} \tag{2.21}$$

Hence

$$\langle i\partial_{\mathbb{X}}\Psi_0\,,\tilde{w}_1\rangle = \langle i\partial_{\mathbb{Y}}\Psi_0\,,\tilde{w}_2\rangle = 0.$$

Thus (2.19) becomes

$$\begin{aligned} \epsilon\dot{q}_x\,\hat{\alpha}_{12} + \dot{q}_y\,(\hat{\alpha}_{11}+\epsilon\hat{\beta}_1) \,&=\, -\gamma_1\,, \\ \dot{q}_x(\hat{\alpha}_{21}+\epsilon\hat{\beta}_2) + \epsilon\dot{q}_y\,\hat{\alpha}_{22} \,&=\, -\gamma_2 \end{aligned} \tag{2.22}$$

where

$$\begin{aligned} &\hat{\alpha}_{11} = \langle i\partial_{\mathbb{Y}}\Psi_0\,,\tilde{w}_1\rangle\,, \quad \hat{\alpha}_{21} = \langle i\partial_{\mathbb{X}}\Psi_0\,,\tilde{w}_2\rangle\,, \quad \hat{\alpha}_{12} = \langle i\partial_{\mathbb{X}}\Psi_1\,,\tilde{w}_1\rangle\,, \\ &\hat{\alpha}_{22} = \langle i\partial_{\mathbb{Y}}\Psi_1\,,\tilde{w}_2\rangle\,, \quad \hat{\beta}_1 = \langle i\partial_{\mathbb{Y}}\Psi_1\,,\tilde{w}_1\rangle\,, \quad \hat{\beta}_2 = \langle i\partial_{\mathbb{X}}\Psi_1\,,\tilde{w}_2\rangle\,, \\ &\eta_j = \langle\hat{N}_\epsilon(\Psi_1),\tilde{w}_j\rangle\,, \end{aligned}$$

and

$$\gamma_j = \hat{\Gamma}_j + \epsilon^2(\langle\Psi_1 H_t,\tilde{w}_j\rangle + \langle i\Psi_{1,t},\tilde{w}_j\rangle) + \eta_j + o_\epsilon\left((\log\frac{1}{\epsilon})^{-1/2}\right)\,.$$

By (2.9), (2.18) and (2.21), we have

$$\begin{aligned} &\hat{\alpha}_{11} = -\tfrac{\pi}{\Gamma_{\epsilon\,1}}\,, && \hat{\alpha}_{21} = \tfrac{\pi}{\Gamma_{\epsilon\,2}}\,, && \\ &\epsilon|\hat{\alpha}_{j\,2}| \le K\epsilon^{1-\beta}\,, && \epsilon|\hat{\beta}_j| \le K\epsilon^{1-\beta}\,, && 0<\beta<1\,, \\ &|\eta_j| = o_\epsilon\left((\log\tfrac{1}{\epsilon})^{-1/2}\right)\,, && \gamma_j = \hat{\Gamma}_j + o_\epsilon\left((\log\tfrac{1}{\epsilon})^{-1/2}\right)\,, && j=1,2\,, \end{aligned} \tag{2.23}$$

where $\Gamma_{\epsilon\,1} = \|\partial_{\mathbb{X}}\Psi_0\|_{L^2}$ and $\Gamma_{\epsilon\,2} = \|\partial_{\mathbb{Y}}\Psi_0\|_{L^2}$. Furthermore, (2.22) implies

$$\dot{q}_x\,(t) = -\frac{1}{\hat{\gamma}}[(\hat{\alpha}_{11}+\epsilon\hat{\beta}_1)\gamma_2 \,-\, \epsilon\hat{\alpha}_{22}\gamma_1]\,, \quad \dot{q}_y\,(t) = -\frac{1}{\hat{\gamma}}[(\hat{\alpha}_{21}+\epsilon\hat{\beta}_2)\gamma_1 \,-\, \epsilon\hat{\alpha}_{12}\gamma_2]\,, \tag{2.24}$$

where $\hat{\gamma} = (\hat{\alpha}_{11}+\epsilon\hat{\beta}_1)(\hat{\alpha}_{21}+\epsilon\hat{\beta}_2) \,-\, \epsilon^2\hat{\alpha}_{12}\hat{\alpha}_{22}$. Moreover, by (2.9), (2.21) and the mean-value theorem of harmonic functions, we have

$$\epsilon\,\langle\Psi_0 H_t\,,\tilde{w}_j\rangle = \frac{\pi\,\epsilon^2}{\Gamma_{\epsilon\,j}}\,\left(\int_0^{\frac{1}{\epsilon}}\, s^2 f_0 f_0'\,ds\right)\,\partial_{x_j}H_t(\mathrm{q}\,,\mathrm{t}\,,\epsilon)\,, \tag{2.25}$$

where $x_1 = x, x_2 = y$. From (1.7) and (1.3), we obtain that

$$\int_0^{\frac{1}{\epsilon}} s^2 f_0 f_0' \, ds = \log \frac{1}{\epsilon} + O(1) . \tag{2.26}$$

Furthermore by (2.9), (2.21), and the mean-value theorem of harmonic functions, we have

$$\begin{aligned}
&\langle i \, \partial_{X_j} \Psi_0 \, \partial_{x_j} H \, , \tilde{w}_j \rangle = 0 \, , j = 1, 2 \, , \\
&\langle i \, \partial_{X_1} \Psi_0 \, \partial_{x_1} H \, , \tilde{w}_2 \rangle = \tfrac{\pi}{\Gamma_{\epsilon\, 2}} \, \partial_{x_1} H(\mathrm{q} \, , \mathrm{t} \, , \epsilon) \, \mathrm{f}_0^2(\tfrac{1}{\epsilon}) \, , \\
&\langle i \, \partial_{X_2} \Psi_0 \, \partial_{x_2} H \, , \tilde{w}_1 \rangle = -\tfrac{\pi}{\Gamma_{\epsilon\, 1}} \, \partial_{x_2} H(\mathrm{q} \, , \mathrm{t} \, , \epsilon) \, \mathrm{f}_0^2(\tfrac{1}{\epsilon}) \, , \\
&|\epsilon \, \langle \Psi_0 | \nabla H|^2 \, , \tilde{w}_j \rangle| \ \leq \ \tfrac{\epsilon C}{\Gamma_{\epsilon\, j}} \, , \quad C = 2\pi K^2 \sup_{0<\epsilon<1} \int_0^{\frac{1}{\epsilon}} s f_0 f_0' \, ds > 0 \, , \\
&\epsilon \, \langle i \, \Psi_0 H_t \, , \tilde{w}_1 \rangle \ = -\tfrac{\pi}{\Gamma_{\epsilon\, 1}} \, \left(\epsilon^2 \, \textstyle\int_0^{\frac{1}{\epsilon}} \, s f_0^2 \, ds \right) \, \partial_{x_2} H_t(\mathrm{q} \, , \mathrm{t} \, , \epsilon) \, , \\
&\epsilon \, \langle i \, \Psi_0 H_t \, , \tilde{w}_2 \rangle \ = \tfrac{\pi}{\Gamma_{\epsilon\, 2}} \, \left(\epsilon^2 \, \textstyle\int_0^{\frac{1}{\epsilon}} \, s f_0^2 \, ds \right) \, \partial_{x_1} H_t(\mathrm{q} \, , \mathrm{t} \, , \epsilon) \, ,
\end{aligned} \tag{2.27}$$

where $X_1 = \mathbb{X}, X_2 = \mathbb{Y}, x_1 = x, x_2 = y$. Hence by (2.20), (2.25), (2.26) and (2.27), we obtain

$$\begin{aligned}
\hat{\Gamma}_1 \ &= \tfrac{\pi}{\Gamma_{\epsilon\, 1}} [2 \partial_y H(\mathrm{q} \, , \mathrm{t} \, , \epsilon) + 2 \, \alpha_0 \, \mathrm{q_x} \\
&\quad + \epsilon^2 (\log \tfrac{1}{\epsilon} + O(1)) \partial_x H_t(\mathrm{q} \, , \mathrm{t} \, , \epsilon) + \mathrm{o}_\epsilon(1)] \, , \\
\hat{\Gamma}_2 \ &= \tfrac{\pi}{\Gamma_{\epsilon\, 2}} [-2 \partial_x H(\mathrm{q} \, , \mathrm{t} \, , \epsilon) + 2 \, \beta_0 \, \mathrm{q_y} \\
&\quad + \epsilon^2 (\log \tfrac{1}{\epsilon} + O(1)) \partial_y H_t(\mathrm{q} \, , \mathrm{t} \, , \epsilon) + \mathrm{o}_\epsilon(1)] \, .
\end{aligned} \tag{2.28}$$

For the terms of α_0 and β_0 in (2.28), we have used

$$\alpha_\epsilon = \epsilon^{-2} \, \left(\log \frac{1}{\epsilon} \right)^{-1} \, (\alpha_0 + o_\epsilon(1)) \, , \quad \beta_\epsilon = \epsilon^{-2} \, \left(\log \frac{1}{\epsilon} \right)^{-1} \, (\beta_0 + o_\epsilon(1)) \, ,$$

the third term of (2.18), and the fact that

$$\begin{aligned}
\langle \mathbb{X} \Psi_0 \, , \tilde{w}_1 \rangle &= \frac{\pi}{\Gamma_{\epsilon\, 1}} \, \left(\log \frac{1}{\epsilon} + O(1) \right) \, , \\
\langle \mathbb{Y} \Psi_0 \, , \tilde{w}_2 \rangle &= \frac{\pi}{\Gamma_{\epsilon\, 2}} \, \left(\log \frac{1}{\epsilon} + O(1) \right) \, , \\
\langle \mathbb{X} \Psi_0 \, , \tilde{w}_2 \rangle &= \langle \mathbb{Y} \Psi_0 \, , \tilde{w}_1 \rangle = 0 \, , \\
\langle \Psi_0 \, , \tilde{w}_j \rangle &= \langle \mathbb{X}^2 \Psi_0 \, , \tilde{w}_j \rangle = \langle \mathbb{Y}^2 \Psi_0 \, , \tilde{w}_j \rangle = 0 \, , j = 1, 2 \, .
\end{aligned}$$

Thus by (2.9), (2.23), (2.24), and (2.28), we obtain

$$\begin{aligned}
\dot{\mathrm{q}}_x \ &= 2 \partial_x \, H(\mathrm{q} \, , \mathrm{t} \, , \epsilon) \ - 2 \beta_0 \, \mathrm{q_y} \, , \\
\dot{\mathrm{q}}_y \ &= 2 \partial_y \, H(\mathrm{q} \, , \mathrm{t} \, , \epsilon) \ + 2 \alpha_0 \, \mathrm{q_x} \, .
\end{aligned} \tag{2.29}$$

Remark 1. Suppose H is a constant function. Then (2.29) becomes

$$\dot{\mathrm{q}}_x = -2 \beta_0 \, \mathrm{q_y} \, , \quad \dot{\mathrm{q}}_y = 2 \alpha_0 \, \mathrm{q_x} \, . \tag{2.30}$$

Hence

$$\mathrm{q_x} = \mathrm{A}\,\cos\left(2\sqrt{\alpha_0\beta_0}\,\mathrm{t}\right) + \mathrm{B}\,\sin\left(2\sqrt{\alpha_0\beta_0}\,\mathrm{t}\right),$$
$$\mathrm{q_y} = \sqrt{\alpha_0/\beta_0}\,\left[\mathrm{A}\,\sin\left(2\sqrt{\alpha_0\beta_0}\,\mathrm{t}\right) - \mathrm{B}\,\cos\left(2\sqrt{\alpha_0\beta_0}\,\mathrm{t}\right)\right],$$

where A and B are constants determined by the initial data $\mathrm{q_x}(0)$ and $\mathrm{q_y}(0)$. This is consistent with the result in [Lundh, 2000] and [Svidzinsky & Fetter, [preprint]].

For the motion of d-vortices, we restrict (1.1) on the vortex cores $B_{r_0}(q_j)$'s and we consider the following system of equations.

$$\begin{cases} -i\,u_t = \Delta u - V_\epsilon(x,y)\,u + \frac{1}{\epsilon^2}\,(1-|u|^2)\,u & \text{for } (x,y) \in B^j_{r_0}(t),\ t>0, \\ u|_{t=0} = u_{j\,0}(x) & \text{for } (x,y) \in B^j_{r_0}(0)\,, \end{cases} \tag{2.31}$$

where $(x,y) = q_j(t) = (q_{jx}(t), q_{jy}(t))$ is the j-th vortex trajectory, q_j is smooth in t, $|q_j - q_k| > 2r_0$ for $j \neq k$, and $B^j_{r_0}(t) \equiv \{(x,y) : |(x,y) - q_j(t)| < r_0\}$ is the j-th vortex core which moves along with the j-th vortex trajectory $(x,y) = q_j(t), j = 1, \cdots, d$. Now we assume that

$$\mathbb{X}^j = \frac{x - q_{jx}(t)}{\epsilon}\,, \quad \mathbb{Y}^j = \frac{y - q_{jy}(t)}{\epsilon}\,, \quad \Psi(\mathbb{X}^j, \mathbb{Y}^j, t, \epsilon) = u(x,y,t,\epsilon) \tag{2.32}$$

for $(x,y) \in B^j_{r_0}$, i.e., $(\mathbb{X}^j, \mathbb{Y}^j) \in B_{r_0/\epsilon}(0)\,, j = 1, \cdots, d$. As for (2.6), we take a similar expansion form of Ψ on each vortex core as follows.

$$\Psi(\mathbb{X}^j, \mathbb{Y}^j, t, \epsilon) = \Psi_0(\mathbb{X}^j, \mathbb{Y}^j)\,e^{i\,H_j} + \epsilon\,\Psi_1(\mathbb{X}^j, \mathbb{Y}^j, t, \epsilon)\,e^{i\,H_j} \ \text{ for } (\mathbb{X}^j, \mathbb{Y}^j) \in B_{r_0/\epsilon}(0)\,, \tag{2.33}$$

where

$$\Psi_0(\mathbb{X}^j, \mathbb{Y}^j) = f_0(R_j) e^{i\,n_j\,\phi_j}\,, \quad n_j \in \{\pm 1\}\,, \quad R_j = |(\mathbb{X}^j, \mathbb{Y}^j)|, \quad \phi_j = \arg(\mathbb{X}^j, \mathbb{Y}^j)\,.$$

Here we assume that

$$\begin{cases} H_j = \sum\limits_{k \neq j} n_k\,\phi_k + H\,, \Delta H = 0 & \text{for } (x,y) \in B_{r_0}(q_j(t))\,, t>0\,, j = 1, \cdots, d\,, \\ |\nabla H|\,, |H_t|\,, |\nabla H_t| \leq K & \text{for } (x,y) \in B_{r_0}(q_j(t))\,, t>0\,, \end{cases} \tag{2.34}$$

where $n_k \in \{\pm 1\}$. As for (2.29), we obtain the equations of q_j given by

$$\begin{aligned} \dot{q}_{jx} &= 2\partial_x\,H_j(q_j\,,t\,,\epsilon) - 2\beta_0\,q_{jy}\,, \\ \dot{q}_{jy} &= 2\partial_y\,H_j(q_j\,,t\,,\epsilon) + 2\alpha_0\,q_{jx}\,. \end{aligned} \tag{2.35}$$

Here we require that Ψ_1 satisfies the "small" perturbation conditions on each vortex core $(\mathbb{X}^j, \mathbb{Y}^j) \in B_{\frac{r_0}{\epsilon}}(0)$ as follows.

$$\begin{aligned} &\|\nabla_{(\mathbb{X}^j, \mathbb{Y}^j)}\Psi_1\|_{L^2(B_{\frac{r_0}{\epsilon}}(0))} \leq K\epsilon^{-\beta}\,, && 0<\beta<1\,, \\ &\|\Psi_1\|_{L^6(B_{\frac{r_0}{\epsilon}}(0))} \leq K\epsilon^{-\gamma}\,, && 0<\gamma<\tfrac{1}{3}\,, \\ &\|\Psi_1\|_{L^2(B_{\frac{r_0}{\epsilon}}(0))} = o_\epsilon\left((\log\tfrac{1}{\epsilon})^{\frac{1}{2}}\right)\,, && \\ &\|\Psi_{1\,,t}\|_{L^2(B_{\frac{r_0}{\epsilon}}(0))} \leq K\epsilon^{-\delta}\,, && 0<\delta<2\,, \end{aligned} \tag{2.36}$$

$$
\begin{aligned}
&|\langle \Psi_1 \, , \tilde{e}_m \rangle| && = o_\epsilon \left(\epsilon^{-2} (\log \tfrac{1}{\epsilon})^{1/2} \right) , \quad m = 1, 2 \, , \\
&\sum_{k=2}^{\infty} \sum_{j=1}^{J(k)} \epsilon^2 \lambda_k \, |\langle \Psi_1 \, , \tilde{e}_{m\,,k} \rangle| && = o_\epsilon(1) \, ,
\end{aligned}
\tag{2.37}
$$

$$
\begin{aligned}
&\left| \int_{\partial B_{\frac{r_0}{\epsilon}}(0)} \Psi_1 \cdot \partial_{\vec{n}} \, \tilde{e}_m \right| && = o_\epsilon \left((\log \tfrac{1}{\epsilon})^{-1/2} \right) , \quad m = 1, 2 \, , \\
&\sum_{k=2}^{\infty} \sum_{m=1}^{J(k)} \left| \int_{\partial B_{\frac{r_0}{\epsilon}}(0)} \Psi_1 \cdot \partial_{\vec{n}} \, \tilde{e}_{m\,,k} \right| && = o_\epsilon(1) \, ,
\end{aligned}
\tag{2.38}
$$

where $J(k)$ is the mutliplicity of the eigenvalue λ_k and $K > 0$ is a constant. In particular, suppose $H \equiv 0$. Then (2.35) becomes (1.3) and we complete the proof of (1.3).

Remark 2. Suppose $\alpha_\epsilon \, , \beta_\epsilon = o_\epsilon(\epsilon^{-2} \, (\log \frac{1}{\epsilon})^{-1})$. Then as for (1.3), the asymptotic motion equations of q_j's becomes (1.4). However, suppose

$$
\alpha_\epsilon = \lambda_\epsilon \, \alpha_0 \, , \quad \beta_\epsilon = \lambda_\epsilon \, \beta_0 \, , \quad \lambda_\epsilon \, \epsilon^2 \, \log \frac{1}{\epsilon} \to \infty \, ,
$$

as ϵ goes to zero. Then under a suitable time scale $O(\lambda_\epsilon \, \epsilon^2 \, \log \frac{1}{\epsilon})$, the asymptotic motion equations of q_j's becomes (1.5). Hence there is no interaction between q_j's and the trajectories of q_j's may be same as in Remark 1.

Remark 3. From [Dalfovo & Giorgini, 1999] and [Feder *et al.*, [preprint]], we learned the generalized Bose-Pitaevskii equation given by

$$
-i \, u_t = \Delta u - V_\epsilon(x, y) \, u + i\omega \, (y \, u_x - x \, u_y) + \frac{1}{\epsilon^2} (1 - |u|^2) \, u \ \text{ for } \ (x, y) \in \mathbb{R}^2 \, , t > 0 \, , \tag{2.39}
$$

with the initial data

$$
u|_{t=0} = u_0(x, y) \quad \text{ for } \ (x, y) \in \mathbb{R}^2 \, , \tag{2.40}
$$

where u is a complex-valued order parameter, ϵ is a positive small parameter, and $V_\epsilon(x, y)$ is defined in (1.1). The term $i\omega \, (y \, u_x - x \, u_y)$ appears for Bose-Einstein condensates rotating about the z axis at an angular frequency ω. From physical experiments (cf. Madison *et al.* [2000]), multiple vortices were generated in confined single-component condensates by rotating a weakly anisotropic trap at an angular frequency ω. Hence we may assume that (2.39) is well-posed. As for (1.3), we may derive the motion equation of d vortices q_j's as follows:

$$
\begin{aligned}
n_j \, \dot{q}_{jx} &= -\partial_{q_{jy}} W(q_1, \cdots, q_d) - n_j \, \omega_1 \, q_{jy} \, , \\
n_j \, \dot{q}_{jy} &= \ \ \partial_{q_{jx}} W(q_1, \cdots, q_d) + n_j \, \omega_2 \, q_{jx} \, ,
\end{aligned}
\tag{2.41}
$$

for $j = 1, \cdots, d$, where $\omega_1 = -\omega + 2\beta_0 \, , \omega_2 = 2\alpha_0 - \omega$ and W is defined in (1.6). Note that ω_1, ω_2 can be any real numbers if we suitably choose ω, α_0 and β_0.

3 Numerical Study of Three Vortices

In this Section, we present the numerical experiments on the asymptotic motion equations (1.8) of three vortices q_j's. The equations (1.8) can be rewritten as

$$\begin{cases} \dot{q}_{jx} = -\sum\limits_{\substack{k=1 \\ k\neq j}}^{3} n_k \frac{q_{jy}-q_{ky}}{|q_j-q_k|^2} - \omega_1 q_{jy}, \\ \dot{q}_{jy} = \quad \sum\limits_{\substack{k=1 \\ k\neq j}}^{3} n_k \frac{q_{jx}-q_{kx}}{|q_j-q_k|^2} + \omega_2 q_{jx}, \end{cases} \tag{3.1}$$

for $j = 1, 2, 3$, where $q_j = q_j(t) = (q_{jx}(t), q_{jy}(t))$ and (ω_1, ω_2) is chosen in the first or third quadrant. For the case $\omega_1 = \omega_2 = 0$, the system (3.1) becomes the standard Kirchhoff problem (cf. Kirchhoff [1883]). From Aref [1979, 1983], we learned that the system (3.1) with $\omega_1 = \omega_2 = 0$ is an integrable system and has either periodic or quasi periodic solution. The system (3.1) with $(\omega_1, \omega_2) \neq 0$ can be regarded as a perturbation of the standard Kirchhoff problem. Hereafter, we set the winding numbers n_k's as $(n_1, n_2, n_3) = (1, 1, 1)$ and $(1, -1, -1)$ for the numerical experiments. From the numerical experiments, we observe that the trajectories of q_j's have chaotic behavior in a bounded region for some (ω_1, ω_2). Furthermore, there are two chaotic trajectories being frequency synchronized [Brown & Kocarev, 2000] and topologically synchronized (see [Afraimovich, 1999; Afraimovich *et al.*, 2000]).

All ODE systems in the following are solved by using ODEABM predictor-corrector solver (http://www.netlib.org/slatec) in a FORTRAN 77 program on a Compaq DS20 workstation with machine double precision $eps \approx 2.22 \times 10^{-16}$. In order to characterize the motion of q_j's we compute (I) Lyapunov exponents, (II) Poincaré maps, (III) Spectrums of waveforms of the system (3.1) with different pairs (ω_1, ω_2). Here we briefly describe (I), (II) and (III) as follows.

(I) Lyapunov exponents: Let $m_1(t), \cdots, m_6(t)$ be the eigenvalues of the transition matrix $\Phi_t(x_0)$ of (3.1) with $\Phi_0(x_0) = \mathrm{I}_6$. The Lyapunov exponents of x_0 are given by

$$\lambda_i(x_0) = \lim_{t\to\infty} \frac{1}{t} |m_i(t)|, \quad i = 1, \cdots, 6, \tag{3.2}$$

whenever the limit exists. Lyapunov exponents are a generalization of the eigenvalues at an equilibrium point of characteristic multipliers. They can be used to determine the stability of quasi-periodic and chaotic behavior as well as that of equilibrium points are periodic solutions. A practical algorithm is developed in FORTRAN 77 according to the pseudo-code in Chapter 3 of Parker & Chua [1989].

(II) Poincaré maps: Poincaré map is a technique to be used to characterized the periodic of quasi K-periodic solution of the ODE system. Let $\mathbb{P} : \sum_5 \to \sum_5$ be the (first) Poincaré map on the 5-dimensional hyperplane $\sum_5$ with the normal vector $v_5 = \overrightarrow{v}(x_\Sigma)$, where $x_\Sigma \in \sum_5$ and $\overrightarrow{v}$ is the vector field of (3.1). It is well known from the numerical point of view that if the points $\mathbb{P}^k(x_\Sigma), k = 1, 2, 3, \cdots$, freeze at one point or densely fill out a closed curve, then the solution of (3.1) forms a periodic solution or a quasi 2-periodic orbit, i.e., two-torus. Otherwise, a second-order Poincaré map is needed to compute which allows an easier

identification of quasi 3-periodic orbit, i.e., 3-torus. (See pp. 43–47 of Parker & Chua [1989].) The sampling of the second-order Poincaré map uses a 4-dimensional hyperplane $\sum_4 \subset \sum_5$ with a suitable normal vector. The points $\mathbb{P}^k(x_\Sigma)$'s that lie on $\sum_4$ make up the orbit of the second-order Poincaré map. In practice, none of the $\mathbb{P}^k(x_\Sigma)$'s lies exactly on $\sum_4$, so those $\mathbb{P}^k(x_\Sigma)$'s within $\varepsilon \approx 10^{-5}$ of $\sum_4$ are collected. If the orbit of the second-order Poincaré map in $\sum_4$ densely fill out a closed curve, then the solution of (3.1) can fairly be said to form a quasi 3-periodic orbit. The extension to higher-order Poincaré maps for quasi K-periodic orbits is obvious. A practical program is written in FORTRAN 77 according to the pseudo-code in Chapter 2 of Parker & Chua [1989].

(III) Spectrums of waveforms: The spectrum of waveform $q(t) \equiv (q_1(t), q_2(T), q_3(t))$ is computed using FFT subroutine in MATLAB and the spectrum distribution is displayed by the frequency versus $\log_{10}(|\mathrm{fft}(q)|_2)$.

3.1 Topological Synchronization

Now we shall introduce the fractal dimension for Poincaré recurrence which can be used as an indicator for topologically synchronized chaotic regimes (see [Afraimovich, 1999; Afraimovich *et al.*, 2000]). Let X, Y be complete metric spaces and $f^t : X \times Y \to X \times Y$ be a dynamical system. Let A be a compact invariant subset of $X \times Y$ and $\pi_1 A = A_1 \subset X, \pi_2 A = A_2 \subset Y$ be the images under natural projections A to X and Y, respectively. Let $U_1 \subset X \cap A_1$ ($U_2 \subset Y \cap A_2$) be an open set in A_1 (A_2), and $x_0 \in U_1$ ($y_0 \in U_2$). Then we may define the number

$$t_1(x_0, U_1) = \inf_{y \in Y_{x_0}} \inf\{t_0(y) | \pi_1 f^{t_0(y)}(x_0, y) \notin U_1\},$$

$$\left(t_2(y_0, U_2) = \inf_{x \in X_{y_0}} \inf\{t_0(x) | \pi_2 f^{t_0(x)}(x, y_0)) \notin U_2\} \right),$$

where $Y_{x_0} = \pi_2(\pi_1^{-1}(x_0) \cap A)$ ($X_{y_0} = \pi_1(\pi_2^{-1}(y_0) \cap A)$). If there exists $\bar{t} > t_1(x_0, U_1)$ ($\bar{t} > t_2(y_0, U_2)$) such that $\pi_1(f^{\bar{t}}(x_0, y)) \in U_1$ for some $y \in Y_{x_0}$ ($\pi_2(f^{\bar{t}}(x, y_0)) \in U_2$ for some $x \in X_{y_0}$), then there is a maximal interval $(\alpha, \beta) \ni \bar{t}$ such that $\pi_1(f^t(x_0, y)) \in U_1$ ($\pi_2(f^t(x, y_0)) \in U_2$) for any $t \in (\alpha, \beta)$. Set

$$t(x_0, U_1) = \begin{cases} 0 & \text{if} \quad t_1(x_0, U_1) = \infty\,, \\ \inf\limits_{y \in Y_{x_0}} \inf \frac{\alpha+\beta}{2} & \text{if} \quad t_1(x_0, U_1) < \infty\,. \end{cases} \tag{3.3}$$

Similarly, introduce

$$t(y_0, U_2) = \begin{cases} 0 & \text{if } t_2(y_0, U_2) = \infty\,, \\ \inf\limits_{x \in X_{y_0}} \inf \frac{\alpha+\beta}{2} & \text{if } t_2(y_0, U_2) < \infty\,. \end{cases} \tag{3.4}$$

Definition 3.1 *The numbers*

$$\tau_x(U_1) = \inf_{x_0 \in U_1} t(x_0, U_1), \quad \tau_y(U_2) = \inf_{y_0 \in U_2} t(y_0, U_2) \tag{3.5}$$

are called the x-Poincaré and y-Poincaré recurrences for U_1 and U_2, respectively.

Definition 3.2 (cf. [Afraimovich *et al.*, 2000]) *A dynamical system $f^t : X \times Y \to X \times Y$ is $\frac{m_0}{n_0}$-topologically synchronized if (i)–(iv) hold as follows:*

(i) It has an attractor A such that nonwandering orbits are dense in A.

(ii) The sets Y_{x_0} and X_{y_0} contain at most N points, respectively, for any $x_0 \in \pi_1(A)$ and $y_0 \in \pi_2(A)$.

(iii) For any $(x_0, y_0) \in A$, there are numbers $\varepsilon_0 > 0$ and $a_1 \geq a_2 \geq 1$ such that: for any open set $U_1 \subset X, U_1 \ni x_0, diamU_1 \leq \varepsilon \leq \varepsilon_0$, there is an open set $U_2 \subset Y, diamU_2 \leq a_1 diamU_1, U_2 \ni y_0$, and for any open set $\widetilde{U}_2 \subset Y, \widetilde{U}_2 \ni y_0, diam\widetilde{U}_2 \leq \varepsilon \leq \varepsilon_0$, there is an open set $\widetilde{U}_1, diam\widetilde{U}_1 \leq a_2 diam\widetilde{U}_2, \widetilde{U}_1 \ni x_0$ such that

$$\tau_y(U_2) = \frac{m_0}{n_0}\tau_x(U_1) + \beta_2, \quad \tau_x(\widetilde{U}_1) = \frac{n_0}{m_0}\tau_y(\widetilde{U}_2) + \beta_1, \tag{3.6}$$

where $m_0, n_0 \in \mathbb{Z}_+$, and β_1, β_2 are bounded as $\varepsilon \to 0$.

(iv) For any set $U_1 \ni x_0$ $(\widetilde{U}_2 \ni y_0), diamU_1 = \varepsilon < \varepsilon_0$ $(diam\widetilde{U}_2 = \varepsilon < \varepsilon_0)$, there are finitely many $x_{0_s} \in U_1$ $(y_{0_s} \in \widetilde{U}_2)$, $s = 1, \cdots, S$, such that

$$\bigcup_{x_0 \in U_1} \bigcup_{y \in Y_{x_0}} U_2(x_0, y) = \bigcup_{s=1}^{S} \bigcup_{y \in Y_{x_{0_s}}} U_2(x_{0_s}, y), \tag{3.7}$$

$$\left(\bigcup_{y_0 \in \widetilde{U}_2} \bigcup_{x \in X_{y_0}} \widetilde{U}_1(x, y_0) = \bigcup_{s=1}^{S} \bigcup_{x \in X_{y_{0_s}}} \widetilde{U}_1(x, y_{0_s}) \right),$$

where $diamU_2(x_0, y_0) \leq a_1\varepsilon$ $(diam\widetilde{U}_1(x, y_0) \leq a_2\varepsilon)$.

Now we consider the sums

$$M_x(\alpha_x, \varepsilon, q) = \inf_{G_1} \sum_k \exp^{-p_x \tau_x(U_{1k})} (\mathrm{diam}U_{1k})^{\alpha_x}, \tag{3.8}$$

$$M_y(\alpha_y, \varepsilon, q) = \inf_{G_2} \sum_k \exp^{-p_y \tau_y(U_{2k})} (\mathrm{diam}U_{2k})^{\alpha_y}, \tag{3.9}$$

where the infimum is taken over all covers G_1 (and G_2) of the set A_1 (and A_2 correspondingly) by open sets with diameters $\leq \varepsilon$. The critical values $p_0^{(x)}$ and $p_0^{(y)}$ satisfying $\alpha_x(p_0^{(x)}) = 0$ and $\alpha_y(p_0^{(y)}) = 0$ in (3.8) and (3.9), respectively are said to be x-and y-Poincaré dimensions for the x-and y-Poincaré recurrences, respectively. We denote

$$\dim_P(A_1) = p_0^{(x)}, \quad \dim_P(A_2) = p_0^{(y)}. \tag{3.10}$$

The following Theorem states the Poincaré dimension for Poincaré recurrences as an indicator of topologically synchronized regimes.

Theorem 3.1 (cf. [Afraimovich, 1999; Afraimovich *et al.*, 2000]) *If a dynamical system* $f^t : X \times Y \to X \times Y$ *is* $\frac{m_0}{n_0}$*-topologically synchronized, then*

$$dim_P(A_2) = \frac{m_0}{n_0} dim_P(A_1). \tag{3.11}$$

The asymptotic equalities of (3.8) and (3.9) show that we may expect

$$\langle \exp\left(-p_0^{(x)} \tau_x(U_{1k}^{\varepsilon})\right)\rangle \sim \varepsilon^{b_1}, \quad \langle \exp\left(-p_0^{(y)} \tau_y(U_{2k}^{\varepsilon})\right)\rangle \sim \varepsilon^{b_2}, \tag{3.12}$$

where $b_i = \dim_B(A_i)$ (box dimension) for $i = 1, 2$, and $\langle\cdot\rangle$ denotes the arithmetic average over k. We may also expect that $b = b_1 = b_2$. In this case (3.12) implies the asymptotic equalities

$$\langle \tau_x(U_{1k}^{\varepsilon})\rangle \sim \frac{-b}{p_0^{(x)}} \ln \varepsilon, \quad \langle \tau_y(U_{2k}^{\varepsilon})\rangle \sim \frac{-b}{p_0^{(y)}} \ln \varepsilon, \tag{3.13}$$

where $\mathrm{diam} U_{1k} \le \varepsilon$ and $\mathrm{diam} U_{2k} \le \varepsilon$.

From the asymptotic equalities of (3.13), $b/p_0^{(x)}$ and $b/p_0^{(y)}$ can be regarded as slopes of straight lines through $(0,0)$ on the $(\langle \tau_x(U_{1k}^{\varepsilon})\rangle, -\ln\varepsilon)$- and $(\langle \tau_y(U_{2k}^{\varepsilon})\rangle, -\ln\varepsilon)$-planes, respectively, for some $0 < \varepsilon_0 \le \varepsilon \le \varepsilon_1 \ll 1$. Thus $b/p_0^{(x)}$ (and $b/p_0^{(y)}$) can be evaluated by the average ratio between $\langle \tau_x(U_{1k}^{\varepsilon})\rangle$ and $-\ln\varepsilon$, ($\langle \tau_y(U_{2k}^{\varepsilon})\rangle$ and $-\ln\varepsilon$) for some different chosen value ε of diameters, e.g. ε from e^{-3} to e^{-2}. From Theorem 3.1 and (3.10) the x- and y-Poincaré dimensions of Poincaré recurrences may serve as indicator for the onset of topologically synchronized chaotic oscillations. This indicator is able to detect the regimes of chaotic synchronization characterized by the frequency ratio $m_0 : n_0$.

3.2 For the case $(n_1, n_2, n_3) = (1, -1, -1)$

We now compute the Lyapunov exponents of the ODE system (3.1) by using ODEABM solver with time-step 0.05 sec. starting with $q_1(0) = (0, 2), q_2(0) = (1, 0)$ and $q_3(0) = (-1, 0)$. The first Lyapunov exponent is computed from 500 sec. to 25000 sec. and plots in Figure 3.1 for $\omega_1, \omega_2 \in (-10, 10)$.

Fig. 3.1 is near here.

From Figure 3.1 we claim that the system (3.1) has a chaotic orbits whenever (ω_1, ω_2) is chosen from the "black" zone in the first quadrant, and fairly has quasi-periodic solution whenever (ω_1, ω_2) is chosen form the "gray" zones in the first and the third quadrants. The "white" zone confirms that the solution of the system (3.1) is unbounded as time goes to infinity.

In Figure 3.2 we plot the chaotic trajectories of three vortices $(q_{jx}(t), q_{jy}(t))$ for $j = 1, 2, 3$, from 25050 sec. to 25100 sec. with $(\omega_1, \omega_2) = (9.88, 2.24)$. The trajectories $q_1(t)$ in red, $q_2(t)$ in blue and $q_3(t)$ in green are bounded and collisionless. The corresponding first Lyapunov exponent is evaluated as 0.4956.

Fig. 3.2 is near here.

Now we compute the second-order Poincaré maps of the system (3.1) with $(\omega_1, \omega_2) = (9.88, 2.24)$. In Figure 3.3 we plot the second-Poincaré maps (4 dim.) projected onto (q_{3x}, q_{3y})-plane. The maps form a fractal pattern. Thus the trajectories of q_j's are fairly said to be chaotic.

Fig. 3.3 is near here.

The spectrum of wave forms of (3.1) with the same (ω_1, ω_2) as above is shown in Figure 3.4.

Fig. 3.4 is near here.

Now we characterized the behavior of trajectories of q_j's insightfully. The vortices $q_j(t)$ $(j = 1, 2, 3)$ are observed to rotate around origin counterclockwisely and clockwisely for $(\omega_1, \omega_2) \in$ I and III, respectively. In Figure 3.5 and 3.6 we plot the trajectories of radius and arguments, respectively, of $q_j(t), j = 1, 2, 3$ with $(\omega_1, \omega_2) = (9.88, 2.24)$. The corresponding spectrums of wave forms are shown in Figure 3.7.

Fig. 3.5, 3.6 and 3.7 are near here.

We denote

$$\nu_j = \max_{s\in[0,1]} \log_{10} |\mathrm{fft}\,(q_j)(s)|, \quad j = 1, 2, 3. \tag{3.14}$$

The following table shows the ratios of ν_1/ν_3 and ν_2/ν_3 with various pairs of (ω_1, ω_2). It is observed that the ratio of ν_2/ν_3 is close to one. Thus, the trajectories of $q_2(t)$ and $q_3(t)$ are fairly said to be "partially" $1:1$-frequency synchronized. The Tabel 3.1 motivates us to study the synchronization behavior between the trajectories of $q_2(t)$ and $q_3(t)$.

Table 3.1. The ratios of ν_1/ν_3 and ν_2/ν_3.

(ω_1,ω_2)	ν_1/ν_3	ν_2/ν_3	ν_3
(9.88,2.24)	1.0624	1.0004	11.0103
(9,10)	1.0564	1.0006	11.5492
(8,6)	1.0552	1.0001	11.4795
(6,1)	1.0562	1.0000	11.1935
(-6,-4)	1.0574	1.0000	11.5438
(-9,-10)	1.0488	1.0000	11.5468
(14,2)	1.0399	1.0000	11.2646

Unfortunately, synchronization regimes between $q_2(t)$ and $q_3(t)$ can not occur in some classical sense. For the case $(\omega_1, \omega_2) = (9.88, 2.24)$, we observe that

No identical synchr. (cf. [31])	$\limsup_{t\to\infty} \lvert q_2(t) - q_3(t)\rvert \neq 0$
No phase synchr. (cf. [32])	$\limsup_{t\to\infty} \lvert \arg(q_2(t)) - \arg(q_3(t))\rvert \neq 0$
No lag synchr. (cf. [33] [1])	$\limsup_{t\to\infty} \lvert q_2(t+\alpha) - q_3(t)\rvert \neq 0$ for any $\alpha > 0$

Let

$$A_j = \{q_j(t) | t \in (1000, 1025)\}, \quad j = 2, 3,$$

for $(\omega_1, \omega_2) = (9.88, 2.24)$. We now recall the asymptotic equality (3.13) and (3.10) for computation of the Poincaré dimensions $\dim_P(A_2)$ and $\dim_P(A_3)$ of the Poincaré recurrence. Choosing $\mathcal{O}_2 = \{U^\varepsilon_{2k}\}$ and $\mathcal{O}_3 = \{U^\varepsilon_{3k}\}$ as open ball coverings of A_2 and A_3, respectively, with various radius ε, we compute the averages of the first return times $\langle \tau_x(U^\varepsilon_{2k})\rangle$ and $\langle \tau_y(U^\varepsilon_{3k})\rangle$ on $\mathcal{O}_2$ and $\mathcal{O}_3$, respectively. Figure 3.8 shows that the plots of $\langle \tau_x(U^\varepsilon_{2k})\rangle$ vs $(-\ln \varepsilon)$ and $\langle \tau_y(U^\varepsilon_{3k})\rangle$ vs $(-\ln \varepsilon)$ calculated for the "q_2 -" and "q_3 -" oscillators have almost the same slopes (ratio=45.0/44.8 $\approx$ 1.0045). From Theorem 3.1 and Figure 3.8 it is fairly said that the chaotic trajectories of $q_2(t)$ and $q_3(t)$ with $(\omega_1, \omega_2) = (9.88, 2.24)$ are $1:1$-topologically synchronized.

Fig. 3.8 is near here.

We now present some numerical evidences of (I) Lyapunov exponents, (II) Poincaré maps, and (III) spectrum of ware form to confirm that the system (3.1) has a quasi 2- or 3-periodic solution for some $(\omega_1, \omega_2) \in (-10, 10)$.

Case (i): Assume $(\omega_1, \omega_2) = (9, 10)$. The bounded and collisionless trajectories of three vortices $q_j(t), j = 1, 2, 3$, form 25080 sec. to 25095 sec. are ploted in Figure 3.9. The Lyapunov exponent is evaluated by 0.000155. The spectrum of wave form from 1000 sec. to 25500 sec. is shown in Figure 3.10. The second-order Poincaré maps from 41179 sec. to 4000000 sec. projected onto (q_{2x}, q_{3x})-plane is ploted in Figure 3.11. The plots of Poincaré maps form two invariant "closed" curves. Note that the fuzzy bands in Figure 3.11 is caused by using a 10^{-5}-neighborhood strategy in computation. Thus the trajectories of q_j's form a quasi 3-periodic solution, i.e., 3-torus, of the system (3.1).

Fig. 3.9, 3.10 and 3.11 are near here.

Case (ii): Assume $(\omega_1, \omega_2) = (6, 1)$. The bounded and collisionless trajectories of q_j's from 25155 sec. to 25190 sec. are ploted in Figure 3.12. The first Lyapunov exponent is evaluated by 0.000236. The spectrum of waveform from 2000 sec. to 25500 sec. is shown in Figure 3.13. The first-order Poincaré maps from 37193 sec. to 1000000 sec. projected onto (q_{1x}, q_{1y})-plane is ploted in Figure 3.14. The plots of Poincaré maps form an invariant closed curve. Thus the trajectories of q_j's form a quasi 2-periodic solution, i.e., 2-torus, of the system (3.1).

Fig. 3.12, 3.13 and 3.14 are near here.

3.3 For the case $(n_1, n_2, n_3) = (1, 1, 1)$

As in subsection 3.2, Figure 3.15 plots the first Lyapunov exponents of the system (3.1) from 500 sec. to 25000 sec. starting with $q_1(0) = (0, 1), q_2(0) = (1, 0)$ and $q_3(0) = (-1, 0)$, for $(\omega_1, \omega_2) \in (-10, 10)$. The "black" and "gray" zones claim that the system (3.1) have chaotic and quasi periodic solutions, respectively. The "white" zone shows that the solution of (3.1) is unbounded as time goes to infinity.

We now present some numerical evidences to illustrate the chaotic and quasi periodic regimes of the system (3.1).

Fig. 3.15 is near here.

Case (iii): Assume $(\omega_1, \omega_2) = (7.40, 0.025)$. We plot trajectories of three vortices $q_j(t), j = 1, 2, 3$, from 2505 sec. to 25070 sec. in Figure 3.16. The first Lyapunov exponent is evaluated by 0.4697. The corresponding Poincaré maps and spectrum of wave form are ploted in Figure 3.17 and 3.18, respectively. The orbit is fairly said to be chaotic.

Fig. 3.16, 3.17 and 3.18 are near here.

We now characterize synchronization behavior of q_j's. The individual spectrum of $q(t), j = 1, 2, 3$, from 2000 sec. to 25500 sec. as shown in Figure 3.19 evaluates the ratios ν_1/ν_3 and ν_2/ν_3 to be 1.0001 and 0.9995, respectively, where ν_j is defined by (3.14).

Fig. 3.19 is near here.

Let

$$A_j = \{q_j(t) | t \in (1000, 1025)\}, \quad j = 1, 2, 3,$$

and let $\mathcal{O}_j = \{U_{jk}^{\varepsilon}\}$ be the open ball covering of A_j, with various radius ε, for $j = 1, 2, 3$. As in subsection 3.2, we compute the average of the first return times $\langle \tau_j(U_{jk}^{\varepsilon}) \rangle$ on $\mathcal{O}_j, j = 1, 2, 3$. Figure 3.20 shows that plots of $\langle \tau_j(U_{jk}^{\varepsilon}) \rangle \; vs \; -\ln \varepsilon$ calculated by "q_j-" oscillator, for $j = 1, 2, 3$ have almost the same slope. The ratio of slopes $= 27.5 : 28.4 : 28.5 \approx 0.97 : 0.9965 : 1$. From Theorem 3.1 and Figure 3.20, it is fairly said that the chaotic trajectories of q_j's with $(\omega_1, \omega_2) = (7.40, 0.025)$ are $1 : 1 : 1$-topologically synchronized. From our numerical experiments, such a topological synchronization is not of identical synchronization, phase synchronization and lag synchronization. In fact, the trajectories of $q_j(t)$ for the case $n_j = 1, j = 1, 2, 3$ behave more complicated than that for the case $(n_1, n_2, n_3) = (1, -1, -1)$.

Fig. 3.20 is near here.

The following Table shows that the ratios of ν_1/ν_3 and ν_2/ν_3 with various pairs (ω_1, ω_2). It is observed that all the ratios are almost close to one. From Brown and Kocarev [2000], the trajectories of q_j's are fairly said to be "partially" $1 : 1 : 1$-frequency synchronized.

Table 3.2. The ratios of ν_1/ν_3 and ν_2/ν_3.

(ω_1, ω_2)	ν_1/ν_3	ν_2/ν_3	ν_3
(0.1,1)	0.9973	0.9926	9.0310
(7.40,0.025)	1.0001	0.9995	11.9722
(-7.79,-1.83)	0.9962	0.9978	9.9978
(-8.46,-1.63)	0.9956	0.9960	9.9799
(-9.80,-1.63)	0.9976	0.9977	10.0885
(8,6)	1.0000	0.9999	10.3570
(-9,-6)	1.0000	1.0000	10.2718

Case (iv): Assume $(\omega_1, \omega_2) = (4, 7)$. The bounded and collisionless trajectories of three vortices $q_j(t), j = 1, 2, 3$, from 25050 sec. to 25085 sec. are plotted in Figure 3.21. The first Lyapunov exponent is evaluated by 0.0043. The second-order Poincaré maps (4 dim.) projected onto (q_{1x}, q_{1y}, q_{3x})-space from 5094 sec. to 4000000 sec. is plotted in Figure 3.22. The plots of Poincaré maps form an invariant closed curve. The fuzzy bands in Figure 3.22 is caused by using a 10^{-5}-neighborhood strategy in computation. The corresponding spectrum of wave form is shown in Figure 3.23. Thus the trajectories of q_j's form a quasi 3-periodic solution, i.e., 3-torus, of the system (3.1).

Fig. 3.21, 3.22 and 3.23 are near here.

4 Conclusions

In this paper, we first derived the asymptotic motion equation of vortices for the time-dependent Gross-Pitaevskii equation with a harmonic trap potential in a two-dimensional Bose-Einstein condensate. The asymptotic motion equations (3.1) can be regarded as a perturbation of standard Kirchhoff problem. We then presented numerical results on the motion of three vortices of (3.1) in a plane for the case with three positive winding numbers as well as with 1 positive and 2 negative winding numbers. Numerical experiments illustrated that the bounded and collisionless trajectories of three vortices form chaotic orbits, quasi 2- or 3-periodic solutions. Furthermore, we observed a new phenomenon of $1:1$-topological synchronization on two chaotic trajectories of vortices with the same sign of winding numbers. In general, this topological synchronization is typically of "partially" $1:1$-frequency synchronization, but not of identical synchronization, phase synchronization and lag synchronization. This provides a further understanding on the dynamics of vortices in two-dimensional Bose-Einstein condensates.

References

[1] Afraimovich, V. S., Verichev, N. N., & Rabinovich, M. I. [1986] *Radiophys. Quantum Electron.* **29**, 747.

[2] Afraimovich, V. S. [1999] "Poincaré recurrences of coupled subsystems in synchronized regimes," *Taiwanese Journal of Mathematics* **3**(2), 139–161.

[3] Afraimovich, V. S., Lin, W. W. & Rulkov, N. F. [2000] "Fractral dimension for Poincaré recurrence as an indicator of synchronized chaotic regimes," *Int. J. Bifurcation and Chaos* **10**(10), 2323–2337.

[4] Aref, H. [1979] "Motion of three vortices," *Phys. Fluids* **22**(3), 393–400.

[5] Aref, H. [1983] "Integrable, chaotic, and turbulent vortex motion in two-dimensional flows," *Ann. Rev. Fluid Mech.* **15**, 345–389.

[6] Bogoliubov, N. N. [1947] *J. Phys. (Moscow)* **11**, 23.

[7] Brown, R. & Kocarev, L. [2000] "A unifying definition of synchronization for dynamical systems," *Chaos* **10** , 344–349.

[8] Chen, X., Elliott, C. M. & Qi, T. [1994] "Shooting method for vortex solutions of a complex-valued Ginzburg-Landau equation," *Proc. Roy. Soci. Edinburgh* **124 A**, 1075–1088.

[9] Dalfovo, F., Giorgini, S., Pitaevskii, L. P. & Stringari, S. [1999] "Theory of Bose-Einstein condensation in trapped gases," *Rev. Mod. Phys.* **71**, 463–531.

[10] Donnelly, R. J. [1991] *Quantized Vortices in Helium II*, (Cambridge Univ. Press, Cambridge).

[11] E, W. [1994] "Dynamics of vortices in Ginzburg-Landau theories with applications to superconductivity," *Physica D.* **77**, 383–404.

[12] Feder, D. L., Clark, C. W. & Schneider, B. I. [1999] "Vortex stability of interacting Bose-Einstein condensates confined in anisotropic harmonic traps," *Phys. Rev. Lett.* **82**, 4956–4959.

[13] Feder, D. L., Svidzinsky, A. A., Fetter, A. L. & Clark, C. W. [preprint] "Anomalous modes drive vortex dynamics in confined Bose-Einstein condensates."

[14] Frisch, T., Pomeau, Y. & Rica, S. [1992] "Transition to dissipation in a model of superflow," *Phys. Rev. Lett.* **69**, 1644–1647.

[15] Ginzburg, V. L. & Pitaevskii, L. P. '[1958] "On the theory of superfluidity," *Sov. Phys. JETP* **7**, 585.

[16] Hagan, P. [1982] "Spiral Waves in Reaction Diffusion Equations," *SIAM J. Appl. Math.* **42**(4), 762–786.

[17] Haraux, A. [1981] "Nonlinear evolution equations- global behavior of solutions," *Lecture Notes in Math.* **841**, (Springer-Verlag, New York.).

[18] Hervé, R. M. & Hervé, M. [1994] "Étude qualitative des solutions réelles d'une équation différentielle liée à l'équation de Ginzburg-Landau," *Ann. Inst. Henri Poincaré* **4**(11), 427–440.

[19] Josserand, C. & Pomeau, Y. [1995] "Generation of vortices in a model superfluid He^4 by the KP instability," *Europhysics Letters* **30**, 43–48.

[20] Kirchhoff, G. [1883] "Vorlesungen über mathematische Physik," *Leipzig: Teubner, vol. 1* Chap. 20, 257.

[21] Landau, L. D. & Lifschitz, E. M. [1989] "Fluid Mechanics," *Course of theoretical physics* **6** (2nd edition, Pergamon press).

[22] Lin, F. H. & Xin, J. X. [1999] "On the incompressible fluid limit and the vortex motion law of the nonlinear Schrödinger equation," *Comm. Math. Phys.* **200**(2), 249–274.

[23] Lin, T. C. [1997] "The stability of the radial solution to the Ginzburg-Landau equation," *Comm. in PDE* **22**, 619–632.

[24] Lin, T. C. [2000] "Spectrum of the linearized operator for the Ginzburg-Landau equation," *Electron. J. Differential Equations* **2000**(42), 1–25.

[25] Lundh, E. & Ao, P. [2000] "Hydrodynamic approach to vortex lifetimes in trapped Bose condensates," *Phys. Rev. A* **61**, 063612(1–7).

[26] Madison, K. W., Chevy, F., Wohlleben, W. & Dalibard, J. [2000] " Vortex formation in a stirred Bose-Einstein condensate," *Phys. Rev. Lett.* **84**, 806–809.

[27] Matthews, M. R., Anderson, B. P., Haljan, P. C., Hall, D. S., Wieman, C. E. & Cornell, E. A. [1999] "Vortices in a Bose-Einstein condensate," *Phys. Rev. Lett.* **83**, 2498–2501.

[28] Neu, J. C. [1990] "Vortices in complex scalar fields," *Physica D.* **43**, 385–406.

[29] Nozieres, P. & Pines, D. [1990] "The theory of quantum liquids," *Vol. II: superfluid bose liquids* (Addison-Wesley Publishing Co., Inc.).

[30] Parker, T. S. & Chua, L. O. [1989] "Practical Numerical Algorithms for Chaotic Systems," (Springer-Verlag).

[31] Percora, L. M. & Carroll, T. L. [1990] "Synchronization in chaotic systems," *Phys. Rev. Lett.* **64**, 821–824.

[32] Rosenblum, M. G., Pikovsky, A. S. & Kurths, J. [1996] "Phase synchronization of chaotic oscillators," *Phys. Rev. Lett.* **76**, 1804–1807.

[33] Rosenblum, M. G., Pikovsky, A. S. & Kurths, J. [1997] "From phase to lag synchronization in coupled chaotic oscillators," *Phys. Rev. Lett.* **78**, 4193–4196.

[34] Svidzinsky, A. A. & Fetter, A. L. [preprint] "Dynamics of a vortex in a trapped Bose-Einstein condensate."

[35] Ting, L. & Klein, R. [1991] "Viscous vortical flows," *Lecture Notes in Physics* **374** (Springer).

[36] http://www.netlib.org/slatec.

Fig. 3.1. The first Lyapunov exponents for $(\omega_1, \omega_2) \in (-10, 10)$ with $(n_1, n_2, n_3) = (1, -1, -1)$.

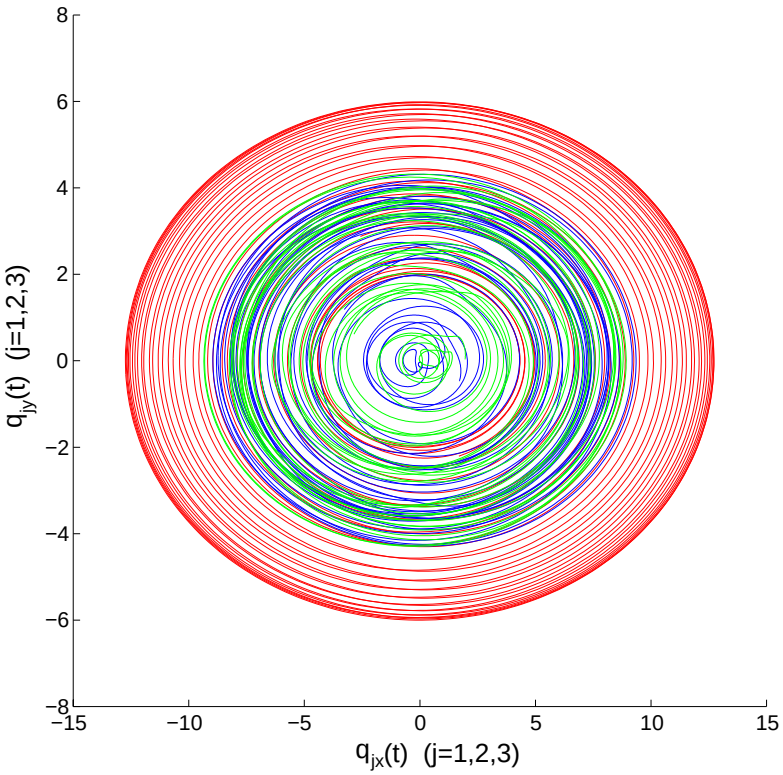

Fig. 3.2. Trajectories of three vortices $q_1(t)$ (in red), $q_2(t)$ (in blue) and $q_3(t)$ (in green) from 25050 sec. to 25100 sec. for a chaotic regime with $(\omega_1, \omega_2) = (9.88, 2.24)$. The 1st Lyapunov exponent is evaluated 0.4956.

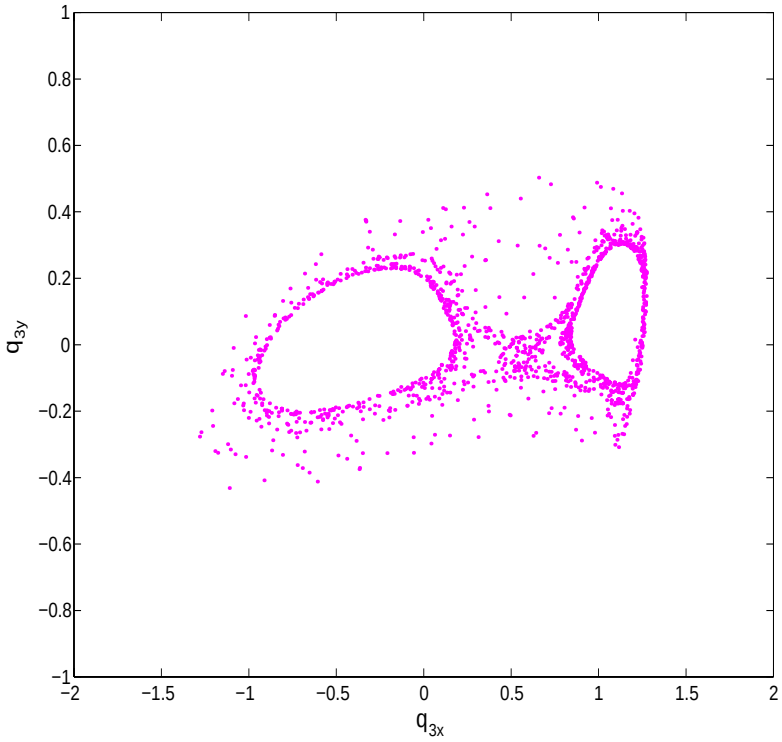

Fig. 3.3. The second-order Poincaré maps (4 dim.) projected onto (q_{3x}, q_{3y})-plane from 1393 sec. to 5000000 sec. for a chaotic regime with $(\omega_1, \omega_2) = (9.88, 2.24)$.

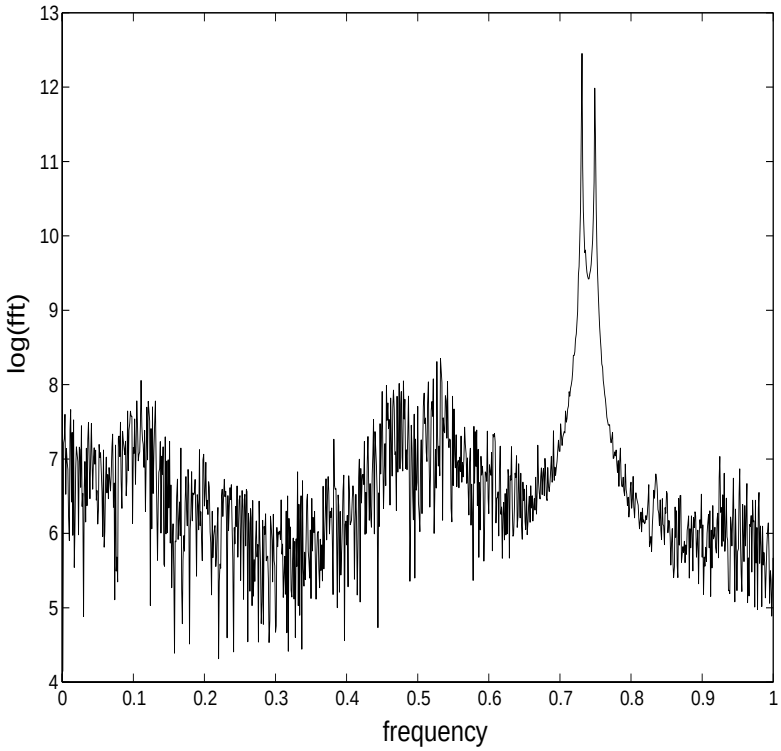

Fig. 3.4. Spectrum of waveforms from 1000 sec. to 25500 sec. for a chaotic regime with $(\omega_1, \omega_2) = (9.88, 2.24)$.

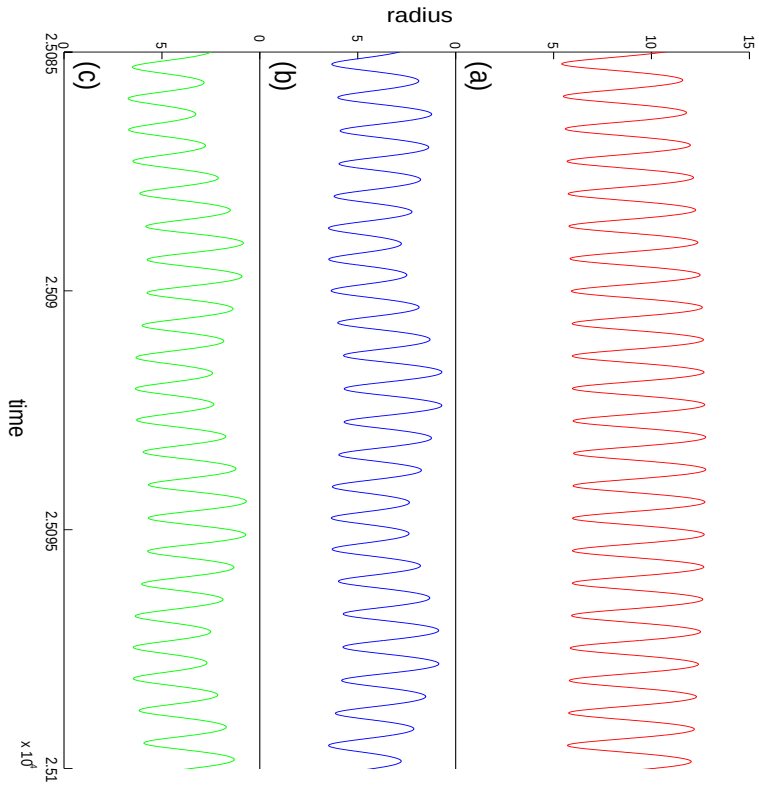

Fig. 3.5. Trajectories of radius for (a) $q_1(t)$, (b) $q_2(t)$ and (c) $q_3(t)$ from 25085 sec. to 25100 sec. with $(\omega_1, \omega_2) = (9.88, 2.24)$.

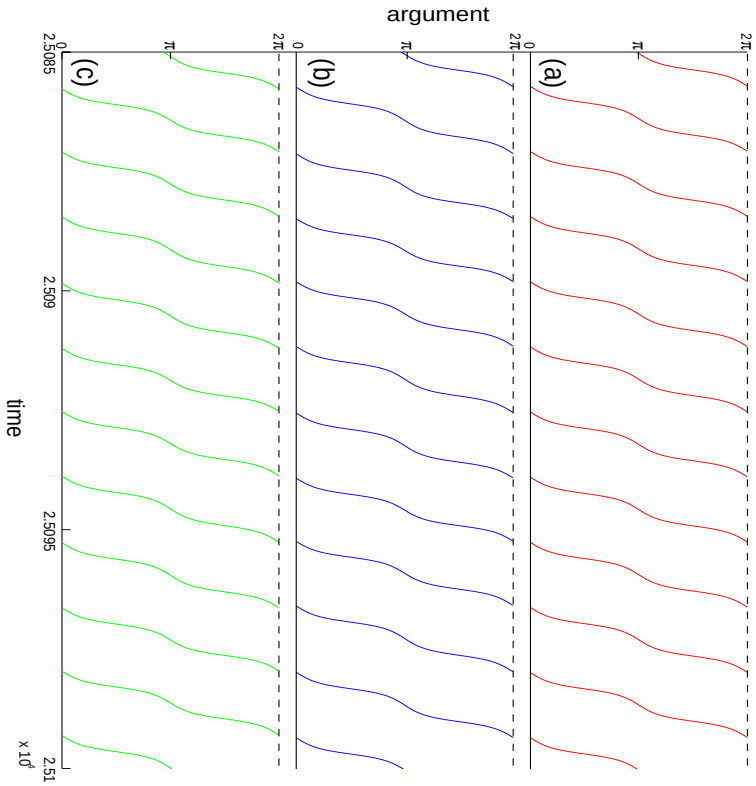

Fig. 3.6. Trajectories of arguments for (a) $q_1(t)$, (b) $q_2(t)$ and (c) $q_3(t)$ from 25085 sec. to 25100 sec. with $(\omega_1, \omega_2) = (9.88, 2.24)$.

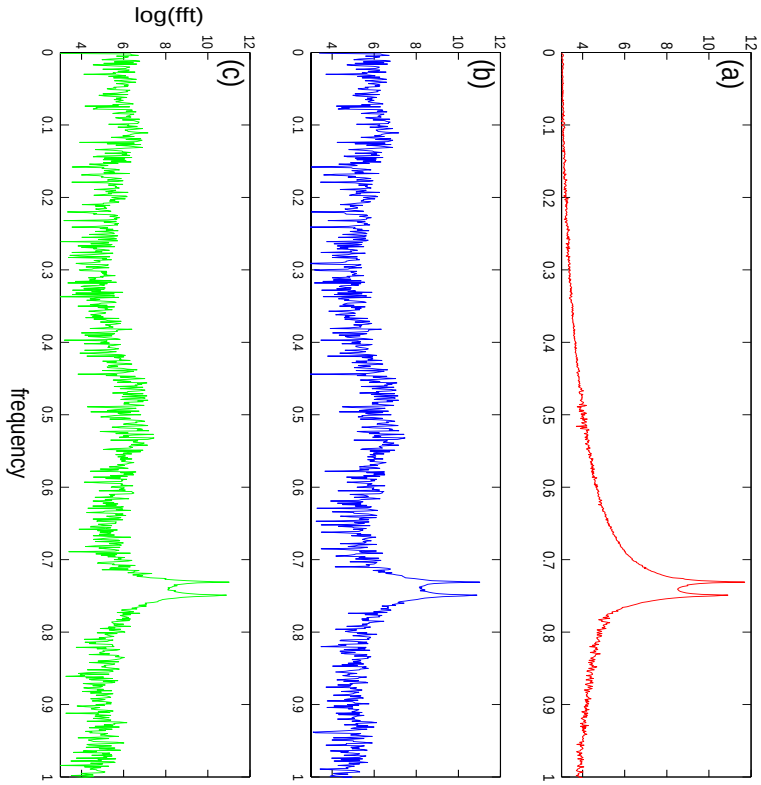

Fig. 3.7. Individual spectrum of (a) $q_1(t)$, (b) $q_2(t)$ and (c) $q_3(t)$ from 1000 sec. to 25500 sec. with $(\omega_1, \omega_2) = (9.88, 2.24)$.

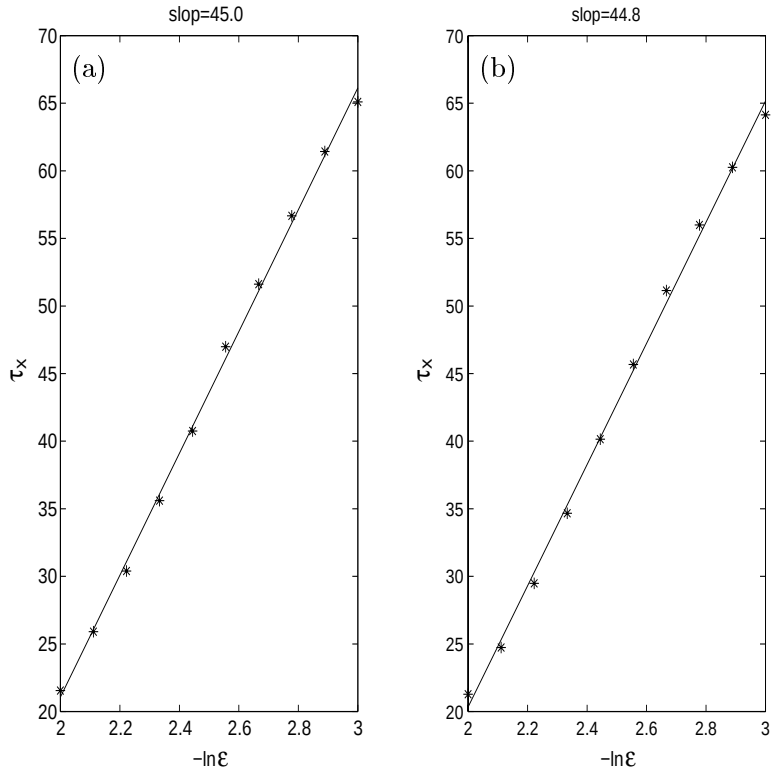

Fig. 3.8. Plots of (a) $\langle \tau_x(U_{2k}^{\varepsilon}) \rangle$ vs $(-\ln \varepsilon)$, (b) $\langle \tau_y(U_{3k}^{\varepsilon}) \rangle$ vs $(-\ln \varepsilon)$ with ε from e^{-3} to e^{-2}. The ratio of slopes $= 45.0/44.8 \approx 1.006$.

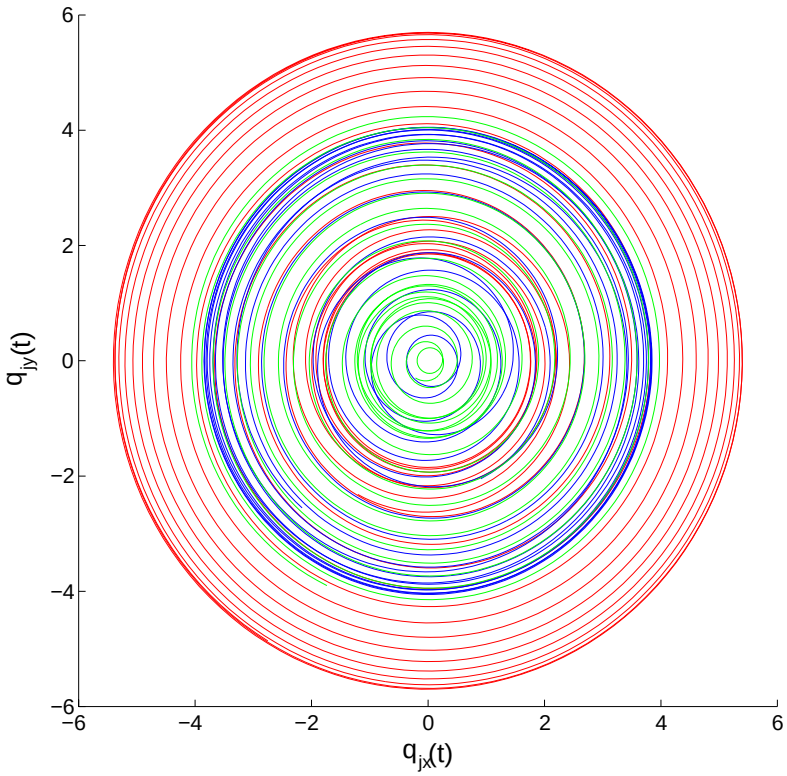

Fig. 3.9. Trajectories of three vortices $q_1(t)$ (in red), $q_2(t)$ (in blue) and $q_3(t)$ (in green) from 25080 sec. to 25095 sec. for a quasi 3-periodic solution with $(\omega_1, \omega_2) = (9, 10)$. The 1st Lyapunov exponent is evaluated 0.000155.

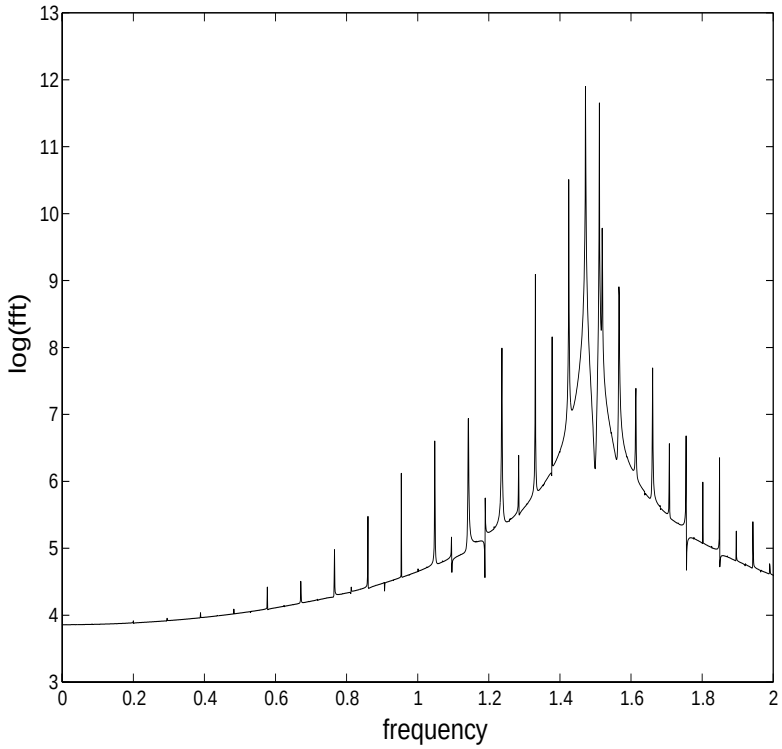

Fig. 3.10. Spectrum of waveforms from 1000 sec. to 25500 sec. for a quasi 3-periodic solution with $(\omega_1, \omega_2) = (9, 10)$.

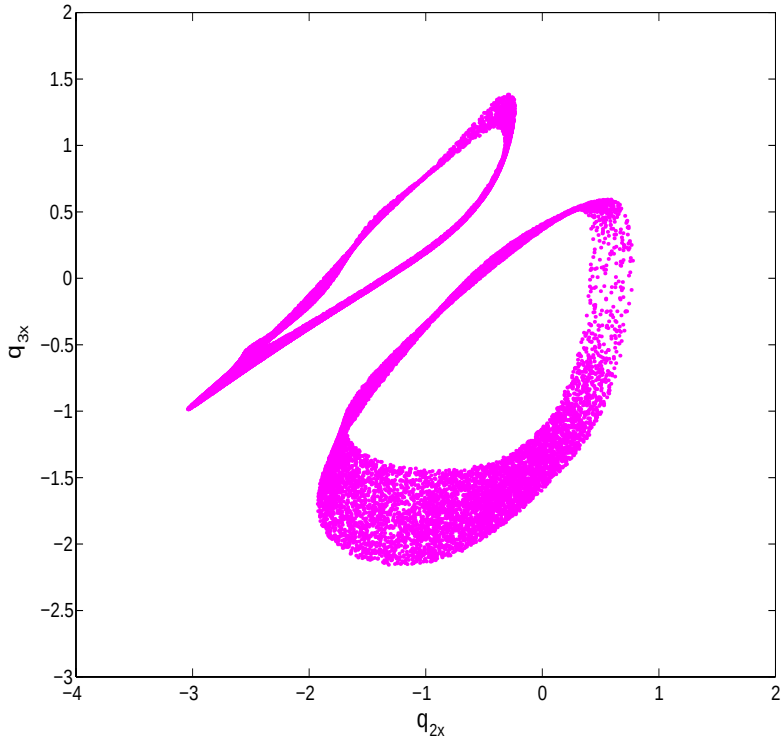

Fig. 3.11. The second-order Poincaré maps (4 dim.) projected onto (q_{2x}, q_{3x})-plane from 41179 sec. to 4000000 sec. for a quasi 3-periodic solution with $(\omega_1, \omega_2) = (9, 10)$.

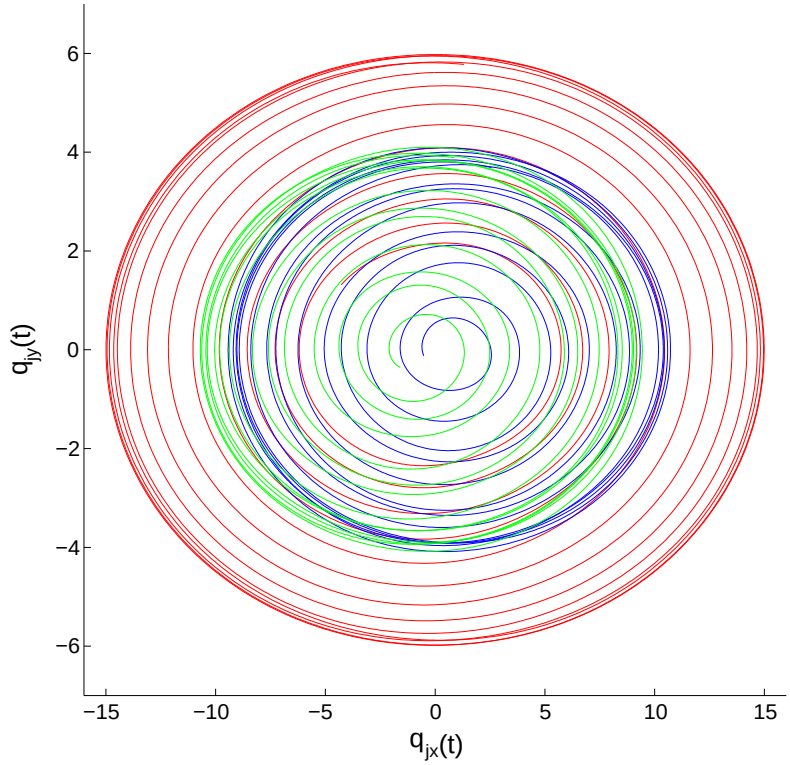

Fig. 3.12. Trajectories of three vortices $q_1(t)$ (in red), $q_2(t)$ (in blue) and $q_3(t)$ (in green) from 25155 sec. to 25190 sec. for a quasi 2-periodic solution with $(\omega_1, \omega_2) = (6, 1)$. The 1st Lyapunov exponent is evaluated 0.000236.

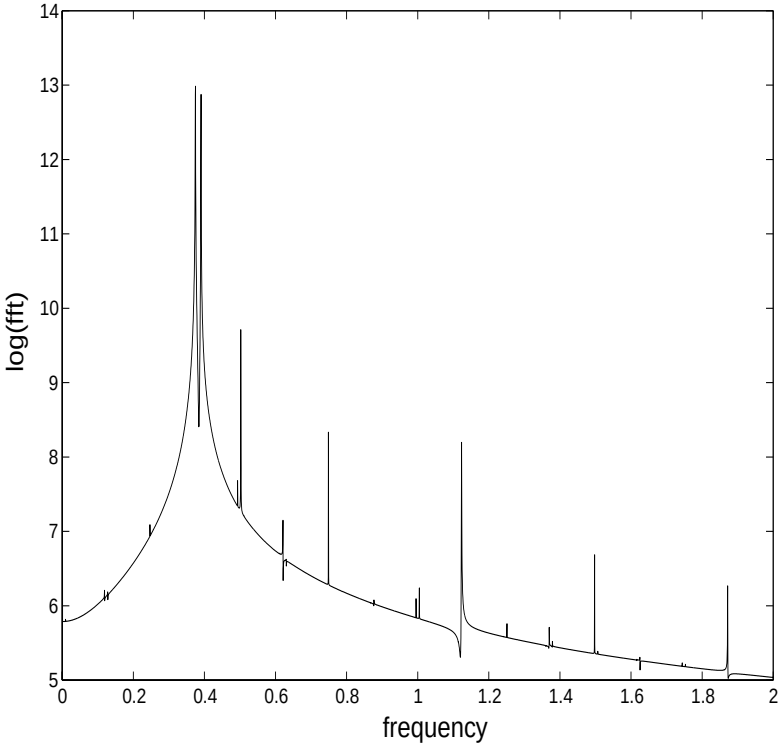

Fig. 3.13. Spectrum of waveforms from 2000 sec. to 25500 sec. for a quasi 2-periodic solution with $(\omega_1, \omega_2) = (6, 1)$.

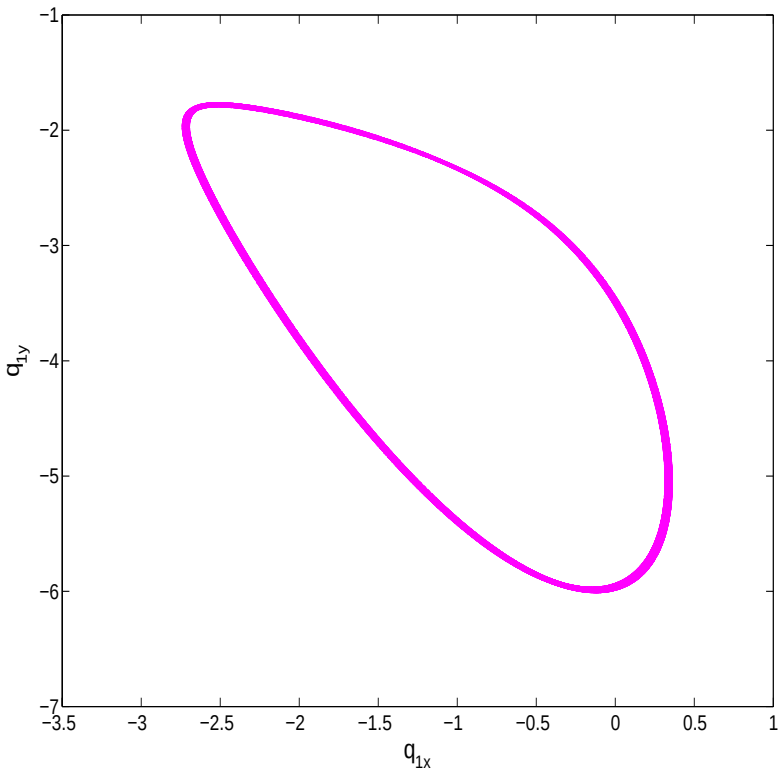

Fig. 3.14. The first-order Poincaré maps (5 dim.) projected onto (q_{1x}, q_{1y})-plane from 37193 sec. to 1000000 sec. for a quasi 2-periodic solution with $(\omega_1, \omega_2) = (6, 1)$.

Fig. 3.15. The first Lyapunov exponents for $(\omega_1, \omega_2) \in (-10, 10)$ with $(n_1, n_2, n_3) = (1, 1, 1)$.

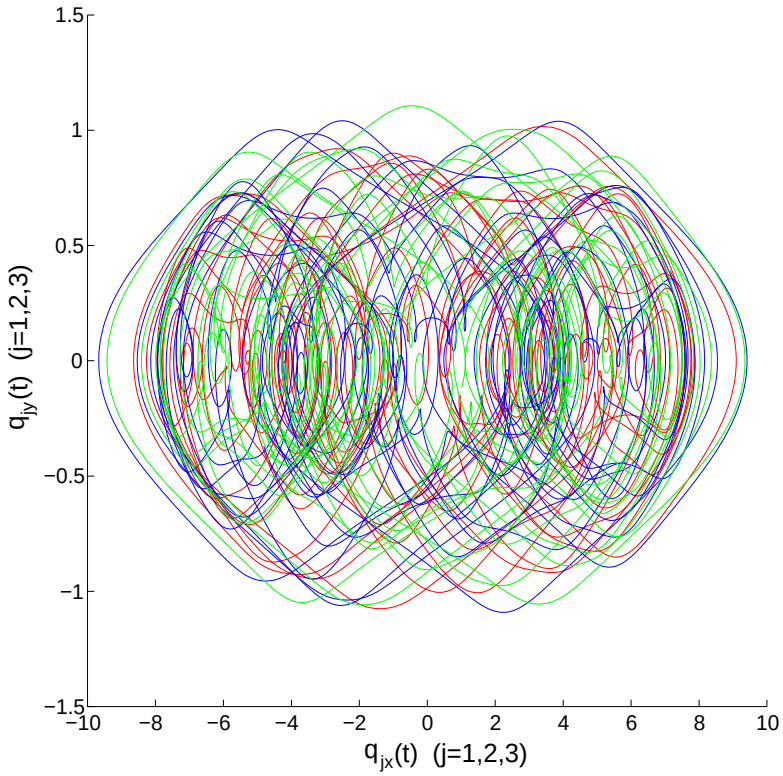

Fig. 3.16. Trajectories of three vortices $q_1(t)$ (in red), $q_2(t)$ (in blue) and $q_3(t)$ (in green) from 25050 sec. to 25070 sec. for a chaotic regime with $(\omega_1, \omega_2) = (7.40, 0.025)$. The 1st Lyapunov exponent is evaluated 0.4697.

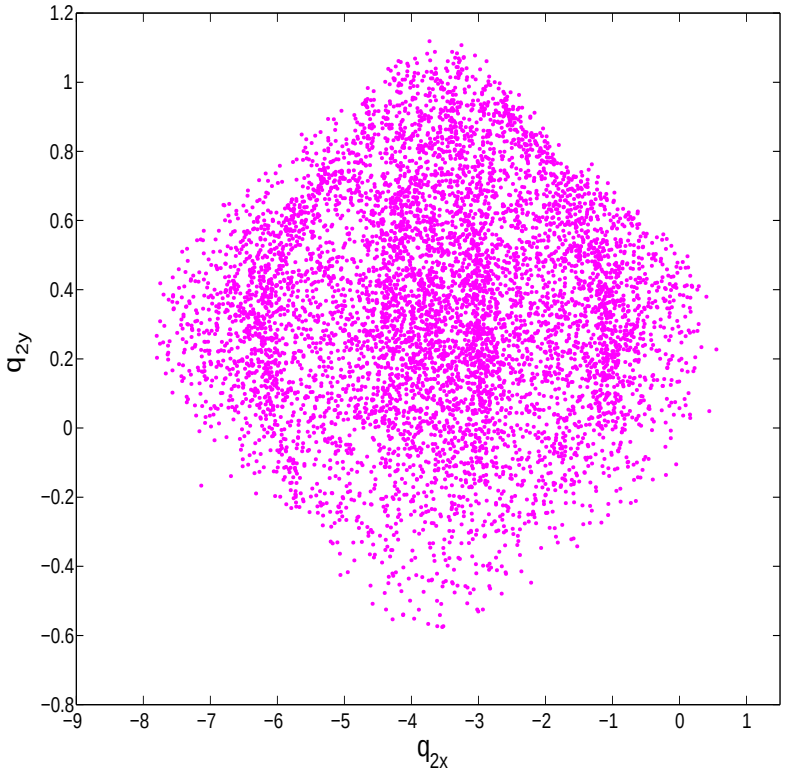

Fig. 3.17. The first-order Poincaré maps (5 dim.) projected onto (q_{2x}, q_{2y})-plane from 1000 sec. to 100000 sec. for a chaotic regime with $(\omega_1, \omega_2) = (7.4, 0.025)$.

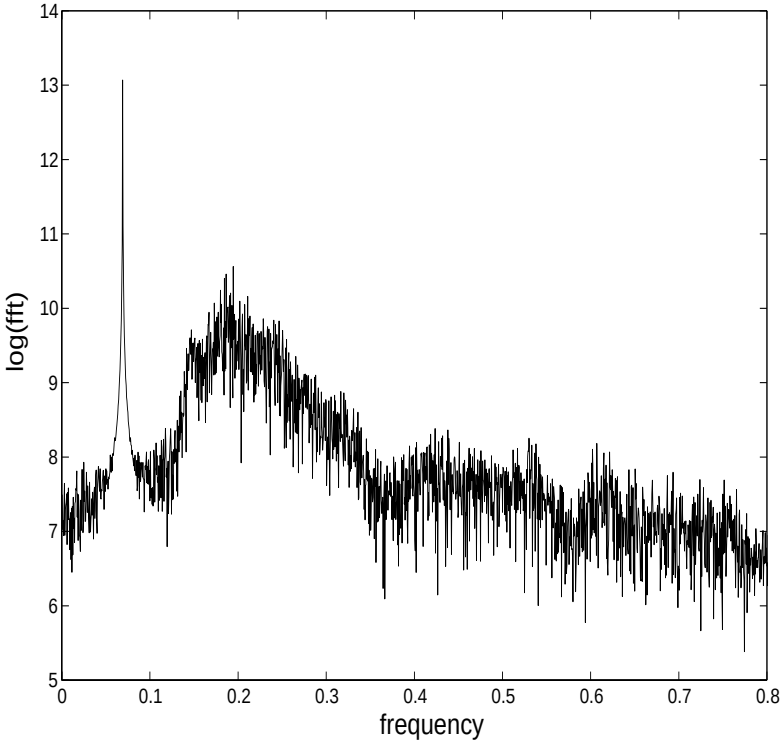

Fig. 3.18. Spectrum of waveforms from 2000 sec. to 25500 sec. for a chaotic regime with $(\omega_1, \omega_2) = (7.4, 0.025)$.

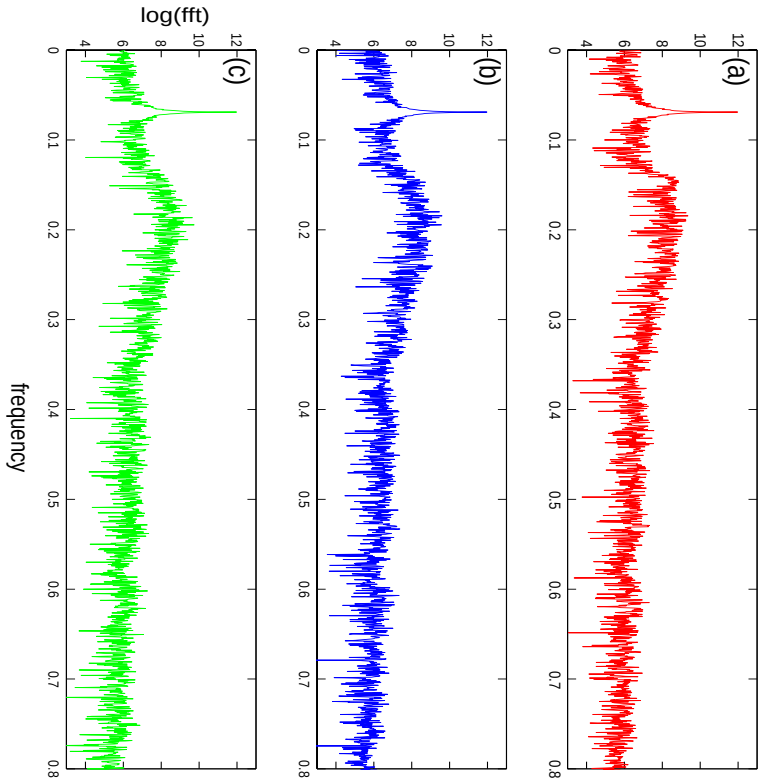

Fig. 3.19. Individual spectrum of (a) $q_1(t)$, (b) $q_2(t)$ and (c) $q_3(t)$ from 2000 sec. to 25500 sec. with $(\omega_1, \omega_2) = (7.40, 0.025)$.

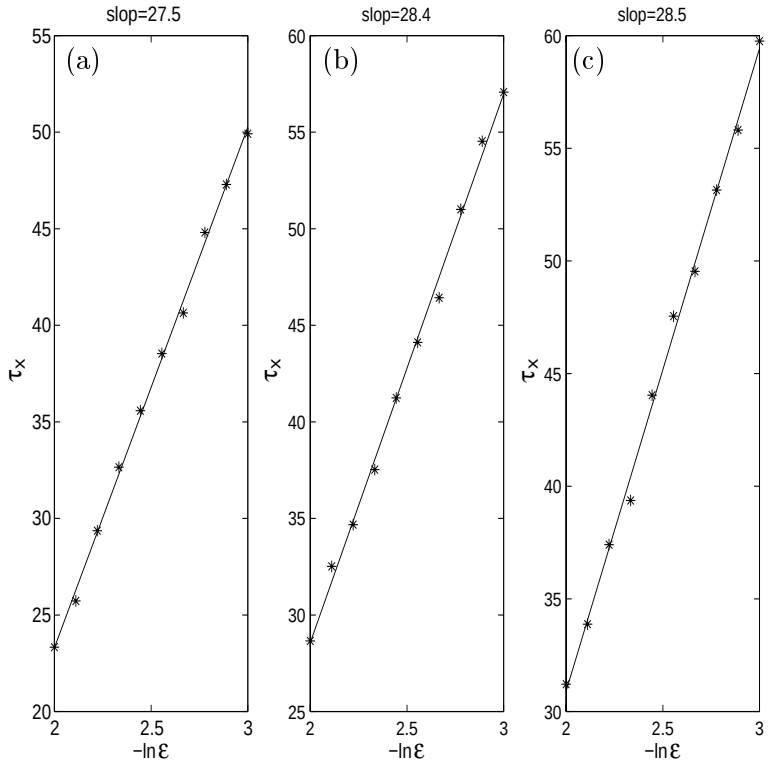

Fig. 3.20. Plots of (a) $\langle \tau_1(U_{1k}^{\varepsilon}) \rangle$ vs $(-\ln \varepsilon)$, (b) $\langle \tau_2(U_{2k}^{\varepsilon}) \rangle$ vs $(-\ln \varepsilon)$, (c) $\langle \tau_3(U_{3k}^{\varepsilon}) \rangle$ vs $(-\ln \varepsilon)$ with ε from e^{-3} to e^{-2}. The ratio of slopes $= 27.5 : 28.4 : 28.5 \approx 0.97 : 0.9965 : 1$.

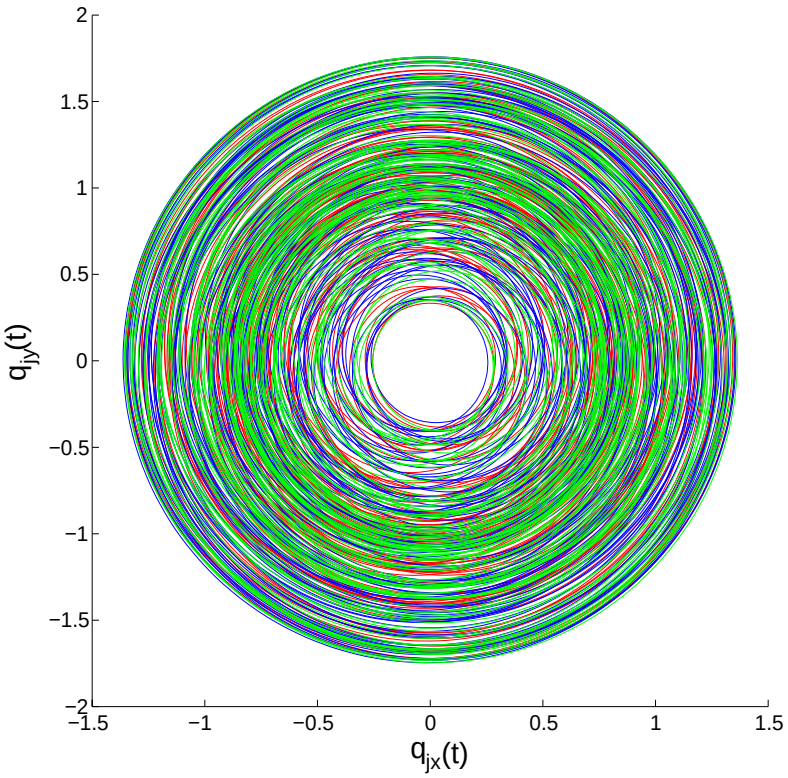

Fig. 3.21. Trajectories of three vortices $q_1(t)$ (in red), $q_2(t)$ (in blue) and $q_3(t)$ (in green) from 25050 sec. to 25085 sec. for a quasi 3-periodic solution with $(\omega_1, \omega_2) = (4, 7)$. The 1st Lyapunov exponent is evaluated 0.0043.

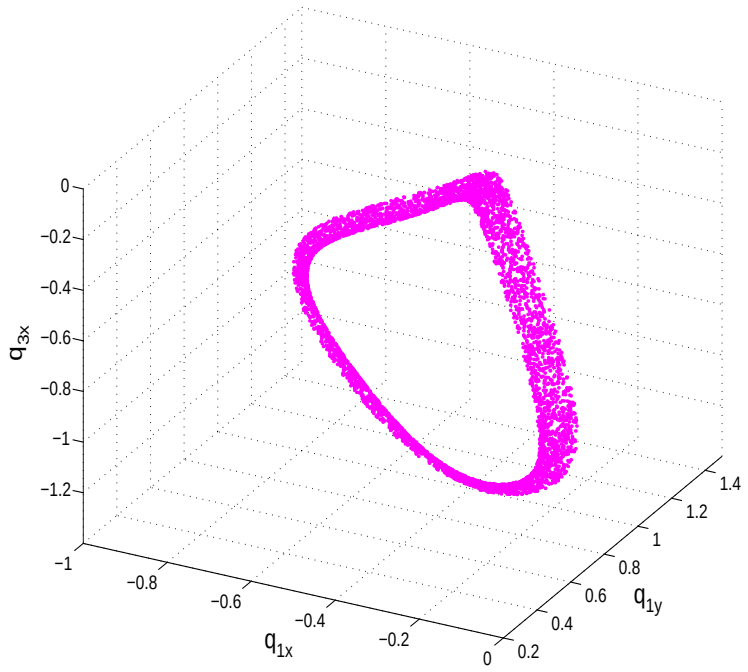

Fig. 3.22. The second-order Poincaré maps (4 dim.) projected onto $(q_{1x}, q_{1y}), q_{3x}$-space from 5094 sec. to 4000000 sec. for a quasi 3-periodic solution with $(\omega_1, \omega_2) = (4, 7)$.

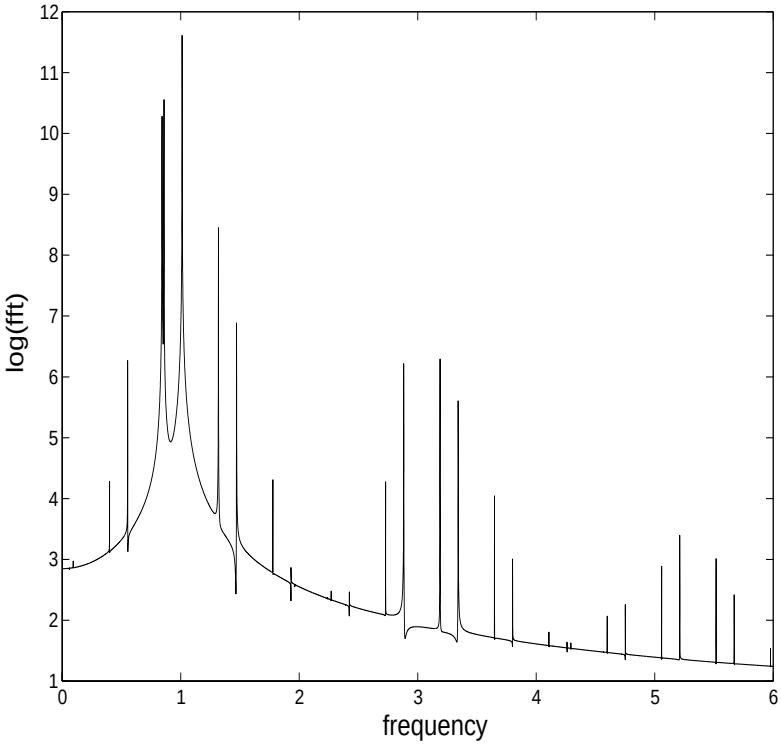

Fig. 3.23. Spectrum of waveforms from 2000 sec. to 25500 sec. for a quasi 3-periodic solution with $(\omega_1, \omega_2) = (4, 7)$.